Supporting information

NMR chemical exchange measurements reveal that N^6-methyladenosine slows RNA annealing

Honglue Shi[1‡], Bei Liu[2‡], Felix Nussbaumer[3], Atul Rangadurai[2], Christoph Kreutz[3*], and Hashim M. Al-Hashimi[1,2*]

[1]Department of Chemistry, Duke University, Durham, NC 27710, USA

[2]Department of Biochemistry, Duke University School of Medicine, Durham, NC 27710, USA

[3]Institute of Organic Chemistry and Center for Molecular Biosciences Innsbruck (CMBI), University of Innsbruck, 6020 Innsbruck, Austria

[‡]These authors contributed equally to this work

**To whom correspondence should be addressed:* hashim.al.hashimi@duke.edu *or* christoph.kreutz@uibk.ac.at

Tel: 919-660-1113

Supplementary Methods

Sample preparation

In what follows we use "ssA_6-DNA(A)" and "ssA_6-DNA(B)" to refer to individual strands but otherwise use "A_6-DNA" when referring to both strands in a duplex (Figure S1).

NMR buffer

All DNA and RNA samples were buffer exchanged with centrifugal concentrators (Amicon Ultra-15 3-kDa cut-off EMD Millipore) into NMR buffer containing 25 mM sodium chloride, 15 mM sodium phosphate, 0.1 mM ethylenediaminetetraacetic acid (EDTA) and 10% D_2O at pH 6.8 with or without 3 mM Mg^{2+}. A subset of CEST data of dsHCV duplexes were collected at a higher concentration of monovalent ions containing 100 mM sodium chloride, 15 mM sodium phosphate, 0.1 mM ethylenediaminetetraacetic acid (EDTA) and 10% D_2O at pH 6.8 with 3 mM Mg^{2+}. The buffer was prepared by mixing equimolar amounts of sodium phosphate mono and dibasic salts, followed by adjusting pH using HCl/NaOH. The final concentrations were ~0.9 mM for A_6-DNA, ~0.8 mM for A_2-DNA, ~1.0 mM for dsGGACU duplexes without Mg^{2+}, ~0.7 mM for dsHCV duplexes with Mg^{2+} at low salt (25 mM sodium chloride) and ~0.4 mM for dsHCV duplexes with Mg^{2+} at high salt (100 mM sodium chloride).

Unlabeled NMR samples

Unmodified DNA oligonucleotide samples (A_2- and A_6-DNA) were purchased from Integrated DNA Technologies (IDT) with standard desalting purification. Unmodified ssGGACU(B) and ssHCV(A) RNA oligonucleotides, and modified ssHCV^{m6A6}(A) were synthesized using a MerMade 6 Oligo Synthesizer using 2′-tBDSilyl and n-acetyl protected A/G/C/U and m^6A phosphoramidites (ChemGenes) and 1 μmol standard synthesis columns (1000 Å) (BioAutomation). RNA oligonucleotides were synthesized with the option to leave the final 5'-protecting group (4,4′-dimethoxytrityl (DMT)) on for 2′-O deprotection and cartridge purification. Synthesized oligonucleotides were cleaved from the 1 μmol columns using 1mL ammonia methylamine (1:1 ratio of 30% ammonium hydroxide and 30% methylamine) followed by 2-hour incubation at room temperature to allow base deprotection. The solution was then air-dried and dissolved in 115 μL DMSO, 60 μL TEA, and 75uL TEA.3HF, followed by 2.5 h incubation at 65 °C for 2′-O deprotection.

The 2′-O deprotected samples were then quenched with Glen-Pak RNA quenching buffer and loaded onto Glen-Pak RNA cartridges (Glen Research Corporation) for purification using the Glen Research online protocol (https://www.glenresearch.com/media/productattach/g/l/glen-pak_2.9_1.pdf). Samples were then ethanol precipitated and air-dried. The DNA strands after purchase and the RNA strands after ethanol precipitation were dissolved in water (200-500 μM for duplex samples) and annealed by heating an equimolar amount of complementary single strands at 95°C for 10 min followed by cooling at room temperature for 2 h. Extinction coefficient for concentration calculation were obtained from the atdbio online calculator (https://www.atdbio.com/tools/oligo-calculator).

Isotopically-labeled NMR samples

The residue-specifically labeled DNA samples were uniformly $^{13}C/^{15}N$-labeled at a specific residues while residue-specifically labeled RNA samples employed nucleotides labeled at specific atoms as indicated in Figure S1. ssA$_6$-DNA^{T9}(A) in which T9 was residue-specifically $^{13}C/^{15}N$-labeled was purchased from Yale Keck Oligonucleotide Synthesis Facility. The sample was purified using Cartridge purification. Site-specifically labeled A$_6$-DNA^{T9} was prepared by annealing ssA$_6$-DNA^{T9}(A) with its unlabeled complementary strand at an equimolar ratio.

Site-specifically labelled ssGGACU^{A6}(A), ssGGACU^{m6A6}(A) and ssHCV^{A15}(B) were synthesized using the same approach used to synthesize unlabelled RNA oligonucleotides described above. ^{13}C8-labeled adenine phosphoramidites were chemically synthesized using the protocol described previously[1]. The ^{13}C2/C8-labeled A/m^{6}A phosphoramidites was chemically synthesized as described below (Figure S6). ssGGACU^{A6}(A), ssGGACU^{m6A6}(A) were ^{13}C8/C2 labeled at A/m^{6}A6 and ssHCV^{A15}(B) was site-specifically ^{13}C8 labeled at A15. The dsGGACU^{A6}, dsGGACU^{m6A6}, dsHCV^{A15} and dsHCV$^{m6A6,\ A15}$ duplexes were prepared by annealing site-specifically labeled strand with their unlabeled complementary strands at equimolar ratio.

The uniformly ^{13}C/^{15}N-labeled ssA$_6$-DNA(A), ssA$_6$-DNA(B) or residue type (G,T or C,A) ^{13}C/^{15}N-labeled ssA$_2$-DNA(A) and ssA$_2$-DNA(B) samples were synthesized by *in vitro* primer extension[2] using a chemically synthesized DNA template (IDT), Klenow fragment DNA polymerase (New England Biolabs) and uniformly ^{13}C, ^{15}N-labeled dNTPs (Sigma-Aldrich). The DNA product was purified using 20% denaturing 29:1 polyacrylamide gel with 8 M urea, 20 mM Tris borate and 1 mM EDTA, then isolated by electro-elution (Whatmann, GE Healthcare) in 40 mM Tris Acetate and 1 mM EDTA and finally ethanol precipitated. All ^{13}C/^{15}N-labeled single stranded DNA were exchanged into NMR buffer and mixed with complementary strands at equimolar ratio to prepare ^{13}C/^{15}N-labeled duplex A$_2$-DNA and A$_6$-DNA samples. The complete formation of a duplex was monitored by looking at disappearance of ^{13}C/^{15}N labeled ss peaks in a 2D [^{13}C, ^{1}H] HSQC experiment at room temperature.

Synthesis of (2,8-^{13}C$_2$)-m^{6}A RNA phosphoramidite

(2-^{13}C)-6-amino-2-thioxo-1,2-dihydro-4(3H)-pyrimidinone (1)

Sodium (1.05 eq, 1.90 g, 82.8 mmol) was dissolved in 60 mL of absolute ethanol under an argon atmosphere. After complete dissolution, ethyl cyanoacetate (1.0 eq, 8.92 g, 78.8 mmol) was added dropwise at room temperature. After 5 min of stirring, ^{13}C-thiourea (1.0 eq, 6.0 g, 78.8 mmol) was added at once and the mixture was refluxed for 2 h, while a white precipitate was formed. The mixture was evaporated, dissolved in 50 mL water and brought to pH 5 with acetic acid after which a white precipitate was formed. Precipitation was completed by storing the mixture 30 min on ice, the solid material was filtered off, washed with a little of water, ethanol and finally with acetone and dried in high vacuum to give **1** as a white solid.

Yield: 11.7 g (quantitative)

^{1}H-NMR (300 MHz, DMSO-d_6, 25°C): δ 11.59 (bs, 1H, N*H*); 11.51 (bs, 1H, N*H*); 6.36 (s, 2H, NH_2); 4,69 (s, 1H, C*H*) ppm.

^{13}C-NMR (75 MHz, DMSO-d_6, 25°C): δ 174.6 (^{13}*C*(2)); 161.6 (*C*(4)); 154.3 (*C*(6)); 78.2 (*C*(5)H) ppm.

(2-^{13}C)-6-amino-5-nitroso-2-thioxo-1,2-dihydro-4(3H)-pyrimidinone (2)

Compound **1** (1.0 eq, 11.7 g, 81.7 mmol) was suspended in 300 mL of 1N HCl. To this a solution of $NaNO_2$ (1.1 eq, 6.20 g, 89.9 mmol) in 28 mL water was added dropwise over a period of 20 min. A red suspension was formed and stirring was continued for 3 h. The solid material was filtered off, washed with a little of water, ethanol and acetone, dried in high vacuum to give **2** as a red solid.

Yield: 14.1 g (quantitative)

^{1}H-NMR (300 MHz, DMSO-d_6, 25°C): δ 7.70 (bs, 2H, NH_2); 11.23 (s, 1H); 12.56 (s, 1H) ppm.

^{13}C-NMR (75 MHz, DMSO-d_6, 25°C): δ 176.4 (^{13}C(2)); 159.8 (C(4)); 143.0 (C(6)); 140.8 (C(5)) ppm.

(2-^{13}C)-5,6-diamino-2-thioxo-2,3-dihydropyrimidin-4(1H)-one (3)

Compound **2** (1.0 eq; 14.0 g; 81.3 mmol) was suspended in 320 mL saturated sodium bicarbonate solution. Sodium dithionite (2.4 eq, 33.9 g, 195 mmol) was added as a solid in 10 portions with stirring at 0°C. Gas evolution and foaming was observed. The mixture was stirred 3 h on ice while the color of the suspension changed from red to yellow. The mixture was brought to pH 7 with acetic acid. The solid material was filtered off, washed with a little of water, ethanol and acetone and dried in high vacuum to give **3** as a yellow solid.

Yield: 12.1 g (76.8 mmol, 94 %)

^{1}H-NMR (300 MHz, DMSO-d_6, 25°C): δ 5.68 (bs, N*H* and NH_2) ppm.

^{13}C-NMR (75 MHz, DMSO-d_6, 25°C): δ 167.5 (^{13}*C*(2)); 157.8 (*C*(4)); 140.4 (*C*(6)); 102.4 (*C*(5)) ppm.

(2-^{13}C)-5,6-diamino-4(3H)-pyrimidinone (4)

Compound **3** (12.1 g, 76.8 mmol) was dissolved in 330mL of 5 % aqueous ammonia. To this was added with stirring 34 g of 50% Raney Nickel, moderate gas evolution was observed. The mixture was refluxed for 2 h. Insoluble material was removed by filtering the hot suspension over a pad of celite. The filter cake was washed with hot water and the filtrate evaporated to dryness to give **4** as a yellow solid.

Yield: 8.04 g (63.6 mmol, 82 %)

^{1}H-NMR (300 MHz, DMSO-d_6, 25°C): δ 7.41 (d, 1H, $^{1}J_{CH}$ = 201.9 Hz, ^{13}C(2)*H*); 5.56 (bs, 2H, NH_2 or N*H*) ppm.

^{13}C-NMR (75 MHz, DMSO-d_6, 25°C): δ 156.2 (*C*(4)); 146.9 (*C*(6)); 138.0 (^{13}*C*(2)); 110.3 (*C*(5)) ppm.

(2,8-^{13}C)-Hypoxanthine (5)

Compound **4** (1.0 eq, 8.0 g, 63.4 mmol) was added in small portions at 40 °C under vigorous stirring to a mixture of 40 mL water and 6.22 g concentrated sulfuric acid (1.0 eq, 6.4 mmol). ^{13}C-formic acid (1.65 eq, 4.81 g, 104.6 mmol) was added at once and the mixture was refluxed overnight to give a red solution. The mixture was cooled to room temperature, concentrated ammonia solution was added to make the solution alkaline and stored at 0°C for 30 min while the product precipitated. The solid was filtered off, washed with a little volume of water, ethanol and acetone. Drying in high vacuum gave **5** as a pale yellow solid.

Yield: 5.60 g (41.2 mmol, 65 %)

^{1}H-NMR (300 MHz, DMSO-d$_6$, 25°C): δ 12.50 (bs, 1H, N*H*); 8.11 (d, 1H, $^{1}J_{CH}$ = 209.9 Hz, ^{13}C(8)*H*); 7.96 (d, 1H, $^{1}J_{CH}$ = 204.7 Hz, ^{13}C(2)*H*) ppm.

^{13}C-NMR (75 MHz, DMSO-d$_6$, 25°C): δ 144.6 (^{13}*C*(2); 140.2 (^{13}*C*(8)) ppm.

5',3',2'-Tri-O-benzoyl-(2,8-^{13}C)-inosine (6)

Compound **5** (1.0 eq, 4.50 g, 33.06 mmol) together with 1-*O*-acetyl-2,3,5-tri-*O*-benzoyl-*β*-*D*-ribofuranose (ATBR, 1.0, 16.70 g, 33.06 mmol) was co-evaporated two times with anhydrous toluene. To the residue suspended in 200 mL of dry toluene was added *N*,*O*-bis(trimethylsilyl)acetamide (BSA, 3.0 eq, 99.2 mmol) under an argon atmosphere. The mixture was refluxed with stirring for 30 min while the suspension turned into a brown solution. To this solution was added trimethylsilyl trifluoromethanesulfonate (TMSOTf, 3.0 eq, 22.0 g, 99.2 mmol) and refluxing was continued for 45 min. Then, thin layer chromatography showed complete conversion. The mixture was evaporated to an oily residue, dissolved in chloroform and washed twice with saturated sodium bicarbonate solution. The organic phase was dried over anhydrous sodium sulfate, filtered and evaporated to dryness. The crude product was applied to a silica gel column with methylene chloride and eluted using a gradient from 0 to 7 % methanol in methylene chloride to give **6** as a yellow foam. The product was dried in high vacuum.

Yield: 12.0 g (20.7 mmol, 63 %)

TLC: CH_2Cl_2/MeOH = 9/1) R_f = 0.6

^{1}H-NMR (300 MHz, DMSO-d_6, 25°C): δ 12.45 (bs, 1H, N*H*); 8.10 (d, 1H, $^1J_{CH}$ = 213,9 Hz, ^{13}C(8)*H*); 7.94 (d, 1H, $^1J_{CH}$ = 207.0 Hz, ^{13}C(2)*H*); 8.00 – 7.45 (m, 15H, C(arom)*H*); 6.56 (m, 1H, C(1')*H*); 6.39 (t, 1H, C(2')*H*); 6.19 (t, 1H, C(3')*H*); 4,87 – 4.63 (m, 3H, C(4')*H*, C(5')H_2) ppm.

^{13}C-NMR (75 MHz, DMSO-d_6, 25°C): δ 165.4 (*C* q); 164.7 (*C* q); 157.2 (*C* q); 146.1 (^{13}*C*(2)); 145.4 (*C* ar); 144.7 (*C* ar); 143.9 (*C* ar); 142.0 (*C* ar); 139.8 (^{13}*C*(8)); 138.7 (*C* ar); 135.5 (*C* q); 133.9 (*C* q); 133.5 (*C* q); 129.4 (*C* ar); 129.7 (*C* ar) 128.74 (*C* ar) 128.70 (*C* ar); 86.5 (*C*(1'); 79.3 (*C*(2'); 73.3 (*C*(3'); 70.6 (*C*(4'); 63.2(*C*(5') ppm.

5',3',2'-Tri-O-benzoyl-(2,8-^{13}C)-6-chloro purine (7)

Compound **6** (1.0 eq, 8.0 g, 13.8 mmol) was dissolved in 80 mL of dry chloroform, thionyl chloride (2.0 eq, 3.28g, 27.6 mmol) was added at once and the mixture was refluxed for 3 h, until thin layer chromatography showed complete conversion. The reaction mixture was cooled to room temperature and quenched by adding it dropwise to a stirred solution of half saturated sodium bicarbonate solution cooled on crushed ice. The two phases were separated and the organic phase was washed once with saturated sodium bicarbonate solution and brine. The organic phase was dried over anhydrous sodium sulfate, filtered and evaporated to dryness. The crude product was applied to a silica gel column with methylene chloride and eluted using a gradient from 0 to 3 % methanol in methylene chloride to give **6** as a colorless foam. The product was dried in high vacuum.

Yield: 5.19 g (8.66 mmol, 62 %)

TLC: CH_2Cl_2/MeOH = 9/1) R_f = 0.8

^{1}H-NMR (300 MHz, DMSO-d$_6$, 25°C): δ 8.94 (d, 1H, $^{1}J_{CH}$ = 218.1 Hz, ^{13}C(8)*H*); 8.65 (d, 1H, $^{1}J_{CH}$ = 210.5 Hz, ^{13}C(2)*H*) 7.98 – 7.43 (m, 15H, C(arom)H); 6.72 (m, 1H, C(1‘)H); 6.49 (t, 1H, C(2‘)H); 6.28 (t, 1H, C(3‘)H); 4.92 – 4.69 (m, 3H, C(4‘)H, C(5‘)H) ppm.
^{13}C-NMR (75 MHz, DMSO-d$_6$, 25°C): δ 165.4 (C q); 164.6 (C q); 164.5 (C q); 151.8 (^{13}C(2)); 146.7 (^{13}C(8)); 145.9 (C ar); 134.0 (C ar); 129.4 (C ar); 128.74 (C ar); 128.68 (C ar); 86.9 (C(1‘)); 79.5 (C(2‘)); 73.1 (C(3‘)); 70.6(C(4‘)); 63.1 (C(5‘)) ppm.

(2,8-^{13}C)-N-6-methyladenosine (8)

Compound **7** (5.19 g, 8.66 mmol) was treated with a 1:1 mixture of 40 mL methylamine solution (33 wt% in absolute ethanol) and 40 mL methylamine solution (40 wt% in water) and stirred at room temperature for 48 h. The mixture was evaporated to dryness and co-evaporated three times with dry ethanol to remove residual water. The residue was dissolved in a minimum of warm methanol and added dropwise to 500 mL of an ice-cooled 1:1 mixture of 500 mL methylene chloride/hexane with vigorous stirring. The precipitated product was filtered off, washed with methylene chloride and dried in high vacuum to give pure **8** as a yellow solid.
Yield: 2.20 g (7.83 mmol, 90 %)
^{1}H-NMR (300 MHz, DMSO-d$_6$, 25°C): δ 8.34 (d, 1H, $^{1}J_{CH}$ = 212.6 Hz, ^{13}C(8)*H*); 8.19 (d, 1H, $^{1}J_{CH}$ = 219.4 Hz, ^{13}C(2)*H*); 5.87 (t, 1H, C(1‘)H); 5.44 (b, 2H, C(2‘)OH, C(5‘)OH); 5.20 (b, 1H, C(3‘)OH); 4.59 (q, 1H, C(2‘)H); 4.14 (b, 1H, C(3‘)H); 3.96 (b, 1H, C(4‘)H); 3.69 – 3.51 (m, 2H, C(5‘)H_2); 2.34 (s, 3H, CH_3) ppm.
^{13}C-NMR (75 MHz, DMSO-d$_6$, 25°C): δ 152.4 (^{13}C(2)); 141.0 (C q); 139.6 (^{13}C(8)); 87.9 (C(1‘)); 85.9 (C(4‘)); 73.5 (C(2‘)); 70.6 (C(3‘)); 61.6 (C(5‘)); 24.2 (CH_3) ppm.

3’,5’-O-bis(t-butylsilyl)-2’-O-(t-butyldimethylsilyl)-(2,8-^{13}C)-N-6-methyladenosine (9)

Compound **8** (1.0 eq, 0.75 g, 2.81 mmol) was dried overnight in high vacuum at 80 °C and then suspended in 15 mL dry DMF and di-*tert*.-butylsilyl bis(trifluoromethanesulfonate) (1.1 eq, 1.36 g, 3.09 mmol) was added dropwise with stirring at 0 °C under an argon atmosphere. After 10 min thin layer chromatography showed complete conversion to the intermediate compound and the suspension turned into a solution. Imidazole (5.0 eq, 0.95 g, 14.1 mmol) was added at once at 0°C and the mixture was allowed to warm to room temperature. *Tert.*-butyl dimethylsilyl chloride (1.2 eq, 0.507 g, 3.37 mmol) was added and the mixture was stirred for 2 h at 60 °C until thin layer chromatography showed complete conversion. DMF was distilled off in high vacuum, the oily residue dissolved in chloroform and washed twice with brine. The organic layer was dried over anhydrous sodium sulfate, filtered, and evaporated to dryness. The crude product was applied to a silica gel column with methylene chloride and eluted using a gradient from 0 to 3 % methanol in methylene chloride to give **9** as a colorless solid. The product was dried in high vacuum.

Yield: 1.01 g (1.87 mmol, 67 %)

TLC: CH_2Cl_2/MeOH = 9/1) R_f = 0.8

^{1}H-NMR (300 MHz, $CDCl_3$, 25°C): δ 8.49 (d, 1H, $^1J_{CH}$ = 201.8 Hz, ^{13}C(8)*H*); 7.73 (d, 1H, $^1J_{CH}$ = 210.47 Hz, ^{13}C(2)*H*); 5.90 (d, 1H, C(1')*H*); 4.62 – 3.99 (5H, C(2')*H*, C(3')*H*, C(4')*H*, C(5')*H*), 3.19 (b, 3H, CH_3), 1.08 – 1.04 (18H, Si(tBu)$_2$, DTBS); 0.92 (9H, Si-tBu, TBDMS); 0.16, 0.14 (6H, Si-$(CH_3)_2$, TBDMS) ppm.

^{13}C-NMR (75 MHz, $CDCl_3$, 25°C): δ 153.4 (^{13}C(2)); 155.5 (^{13}C(8)) ppm.

2'-O-(t-butyldimethylsilyl)-(2,8-^{13}C)-N-6-methyladenosine

Compound **9** (1.0 g, 1.87 mmol) was dissolved in 10 mL of dry methylene chloride. To this solution was added dropwise at 0 °C under stirring a pre-mixed solution of 150 µL HF-pyridine (70 % hydrogen fluoride basis, 30 % pyridine basis) and 900 µL pyridine. After stirring 2 h at 0 °C thin layer chromatography showed complete conversion. The mixture was allowed to warm to room temperature, diluted with chloroform and washed once with saturated sodium bicarbonate solution. The organic layer was dried over anhydrous sodium sulfate, filtered and evaporated to dryness. The crude product was dried in high vacuum and used without further purification for the next step.

TLC: ethyl acetate/n-hexane = 7/3) R_f = 0.1

2'-O-(t-butyldimethylsilyl)-5'-O-(4,4'-dimethoxytrityl)-(2,8-^{13}C)-N-6-methyladenosine (10)

The crude product of the previous step (1.0 eq, 710 mg, 1.80 mmol) together with one spatula tip (catalytic amount) of 4-(dimethylamino)pyridine was co-evaporated twice with anhydrous pyridine and then dissolved in 7 mL of dry pyridine. Then, 4,4'-dimethoxytrityl chloride (1.2 eq, 731 mg, 2.16 mmol) was added in three portions within one hour and the mixture was stirred 3 h at room temperature, thin layer chromatography showed complete conversion. The mixture was quenched with 1 mL of methanol, evaporated to an oily residue and two times co-evaporated with toluene. The residue was dissolved in chloroform and washed two times with 5 % citric acid and once with saturated sodium bicarbonate solution. The organic layer was dried over anhydrous sodium sulfate, filtered and evaporated to dryness. The crude product was applied to a silica gel column with methylene chloride and eluted using a gradient from 0 to 3 % methanol in methylene chloride to give **10** as a yellowish foam. The product was dried in high vacuum.

Yield: 800 mg (1.15 mmol, 61 % referred to **9**)

TLC: ethyl acetate/n-hexane = 7/3) R_f = 0.5

^{1}H-NMR (300 MHz, DMSO-d_6, 25°C): δ 8.26 (d, 1H, $^1J_{CH}$ = 212.3 Hz, ^{13}C(8)*H*); 8.15 (d, 1H, $^1J_{CH}$ = 219.2 Hz, ^{13}C(2)*H*); 7.72 – 6.84 (9H, C(arom)H); 5.96 (t, 1H, C(1')*H*); 5.13 (d, 1H, C(3')O*H*); 4.86 (t, 1H, C(2')*H*); 4.27 (q, 1H, C(3')*H*); 4.11 (q, 1H, C(4')*H*) 3.74(s, 6H, 2 x OCH_3); 3.28 (m, 2H, C(5')H_2)); 2.96 (b, 3H, CH_3); 0.77 (s, 9H, tBu); 0.036, -0,128 (2 x s, 6H, Si(CH_3)$_2$) ppm.

^{13}C-NMR (75 MHz, DMSO-d_6, 25°C): δ 152.60 (^{13}*C*(2)); 139.22 (^{13}*C*(8)); 130.5 (*C* ar); 128.2 (*C* ar); 113.9 (*C* ar); 88.7 (*C*(1')); 84.5 (*C*(4')) 57.8 (*C*(2')); 71.6 (*C*(3')); 64.6 (*C*(5')); 56.1 (O*C*H_3); 27.8 (N*C*H_3); 26.8 (Si-tBu); -3.80 (Si($CH_3)_2$) ppm.

2'-O-(t-butyldimethylsilyl)-5'-O-(4,4'-dimethoxytrityl)-(2,8-^{13}C)-N-6-methyladenosine 3'-[(2-cyanoethyl)-(N,N-diisopropyl)]phosphoramidite (11)

Compound **11** (1.0 eq, 800 mg, 1.15 mmol) was dissolved in 10 mL of dry tetrahydrofuran. To this solution was added simultaneously 2-cyanoethyl-N,N-diisopropylchlorophosphoramidite (CEP-Cl, 2.0 eq, 544 mg, 2.3 mmol) and N,N-diisopropylethylamine (5.0 eq, 740 mg, 5.75 mmol) under an argon atmosphere with stirring. After stirring 2 h at room temperature the reaction mixture was quenched by addition of 1 mL methanol. The mixture was diluted with chloroform and washed once with saturated sodium bicarbonate solution. The organic layer was dried over anhydrous sodium sulfate, filtered and evaporated to dryness. The crude product was applied to a silica gel column with ethyl acetate/n-hexane 2:8 (+ 2 % triethylamine) and eluted using a gradient from 2:8 to 7:3 ethyl acetate/n-hexane (+ 2 % triethylamine) to give **12** as a colorless foam. The product was dried in high vacuum.

Yield: 620 mg (0.69 mmol, 61 %)

TLC: ethyl acetate/n-hexane = 7/3 + 2 % triethylamine) R_f = 0.6

^{1}H-NMR (300 MHz, $CDCl_3$, 25°C): δ 8.29 (d, 1H, $^{1}J_{CH}$ = 200.2 Hz, ^{13}C(8)*H*); 7.96 (d, 1H, $^{1}J_{CH}$ = 209.5 Hz, ^{13}C(2)*H*); 7.48 – 7.21, 6.81 (9H, C(arom)*H*); 5.98 (m, 1H, C(1')*H*); 5.08 (m, 1H, C(2')*H*); 4.41 (b, 1H, C(3')*H*); 4.34 (b, 1H, C(4')*H*); 3.94, 3.65 (m, 2H, PO-CH_2); 3.63 (m, 2H, 2 x N*H*-($CH_3)_2$); 3.77 (s, 6H, 2 x OCH_3); 3.61, 3.31 (m, 2H, C(5')H_2); 2.64, 2.29((2H; CN-CH_2); 1.18 (m, 12H, 2 x NH-(C$H_3)_2$); 0.76 (s, 9H, tBu) ppm.

^{13}C-NMR (75 MHz, $CDCl_3$, 25°C): δ 153.3 (^{13}*C*(2)); 139.1 (^{13}*C*(8)) ppm.

^{31}P-NMR (121 MHz, CDCl3, 25°C): δ 151.6, 149.6 ppm.

NMR experiments

Resonance assignments

All NMR experiments were performed on Bruker Avance III 600 MHz or 700 MHz NMR spectrometers equipped with a 5mm triple-resonance HCN cryogenic probe. Resonance assignments for A_6-DNA, A_2-DNA have been reported previously[3-4]. Resonance assignments for ssA_6-DNA(A) and ssA_6-DNA(B) were obtained using 2D [^{1}H, ^{1}H] NOESY experiments with 350 ms mixing time along with 2D [^{13}C, ^{1}H] and [^{15}N, ^{13}C] HSQC experiments. The assignments for dsGGACU and dsHCV could be readily obtained since the samples were site-specifically labelled.

^{13}C and ^{15}N $R_{1\rho}$ relaxation dispersion

^{13}C and ^{15}N $R_{1\rho}$ experiments were performed on Bruker Avance III 600 MHz or 700 MHz spectrometers as described previously[5]. The spinlock powers and offsets used in the $R_{1\rho}$ experiments are listed in Table S5. R_2(^{13}C) values for the single strands were measured using on resonance $R_{1\rho}$ with high spinlock power (up to 2500 Hz).

Analysis of $R_{1\rho}$ data

Fitted peak intensities determined by NMRpipe[6] at each delay time were fitted to a mono-exponential decay to obtain $R_{1\rho}$ as described previously[5]. Errors in $R_{1\rho}$ were estimated using Monte Carlo simulations. The $R_{1\rho}$ data was fit to 2-state models through numerical integration of the Bloch-McConnell (BM) equations to extract exchange parameters of interest. Model selection ($R_{2,GS}≠R_{2,ES}$ or $R_{2,GS}=R_{2,ES}$, Figure S5) was carried out by calculating Akaike's (w_{AIC}) and Bayesian information criterion (w_{BIC}) weights for each model and selecting the model with the highest relative probability as described previously[7]. In all cases, the selected model was 2-state with $R_{2,GS}≠R_{2,ES}$. We also observed reasonable agreement between the $R_{2,ES}$ values derived from RD and those measured directly for the isolated single-strands though the agreement varied depending on the p_{ss} value used during $R_{1\rho}$ fitting (Figure S5).

^{13}C and ^{15}N CEST

The pulse sequence used for ^{13}C and ^{15}N CEST measurements was obtained by modifying the 1D ^{13}C and ^{15}N $R_{1\rho}$ pulse sequences[8] to remove the pulses required to align magnetization prior to the spin-lock period[9]. The pulses to align water magnetization along its effective field during the relaxation period are also removed, in case of the ^{15}N pulse sequence. The GS magnetization excited by the selective Hartman-Hahn magnetization transfer was not allowed to undergo equilibration prior to the relaxation period. Indeed no minor peaks corresponding to the ES peak in the ^{1}H dimension were observed. A $90_x240_y90_x$ composite pulse of 3300-4000 Hz for ^{13}C and 4000 Hz for ^{15}N is used for ^{1}H decoupling during the relaxation period as described previously[10]. Spin-lock powers were calibrated as described previously[11]. A series of 1D ^{13}C and ^{15}N CEST experiments for each nucleus were recorded for spin-lock power and offset combinations specified in Table S6, using a relaxation delay of 200 ms. For each spin-lock power, the experiment with zero relaxation delay was run in triplicate to obtain error estimates (see below).

Analysis of CEST data

The peak intensity as a function of spin-lock power and offset in the 1D ^{13}C/^{15}N CEST experiments was extracted using NMRPipe[6]. The error in the measured intensity for each spin-lock power was set to be equal to the standard deviation of the measured intensities for a set of triplicate experiments with zero relaxation delay. For each spin-lock power, the intensities were normalized to the average of the intensities recorded for the experiment with zero relaxation time delay and same spin-lock power, which was run in triplicate. The CEST profiles thus obtained were fit to a two state exchange model between ground state (GS) and excited state (ES), by numerically integrating the Bloch-McConnell equations as described previously[9-10]. No equilibration of GS magnetization was assumed when integrating the Bloch-McConnell equations and the spin-lock was also assumed to be perfectly homogenous. The profiles were fit using an in-house python script, by minimizing the deviation χ^2 between the measured (I_{meas}) and predicted (I_{pred}) normalized CEST intensities:

$$\chi^2 = \sum_{i=1}^{N}((I_{meas} - I_{calc})/\sigma_{meas})^2$$

where σ_{meas} is the experimental error and the summation is over all spin-lock power and offset combinations. The relatively high reduced χ^2 observed for a subset of DNA CEST datasets can be attributed to underestimation of the uncertainty using the triplicate method. Indeed, lower reduced χ^2 values are obtained when estimating error based on the intensity variations in the regions of CEST spectra that do not contain any intensity dips, as described by Kay et al[10]. The fitted parameters for individual sites were p_{ss}, k_{ex}, $R_{2,GS}$, $R_{2,ES}$, R_1 and $\Delta\omega$. Global fitting was performed by sharing p_{ss} and k_{ex} for all sites while retaining site-specific $R_{2,GS}$, $R_{2,ES}$, R_1 and $\Delta\omega$ values. The errors in the fitted parameters were estimated by using a Monte-Carlo approach[12]. 100 CEST profiles were generated with the normalized intensity at each spin-lock power offset combination being sampled from a normal distribution with a mean value equal to the measured normalized intensity and standard deviation equal to the estimated error in the normalized intensity. These CEST profiles were then fit to the Bloch-McConnell equations, and the error in the obtained exchange parameters was computed as the standard deviation in the distribution of the fitted parameter. Because the spin-lock power $\omega_1 < k_{ex}$ in the CEST experiment, the k_{-1} values were well determined[13] (Figure S4). The high values of the fitted $R_{2,ES}$ from the CEST data (Table S4) could arise from a more complex exchange topology[14] e.g. GS⇔ES1⇔ES2, in which exchange between GS and ES1 is slow, while that between ES1 and ES2 is relatively faster. Indeed, prior studies[15-16] have proposed a zipper model for nucleic acid annealing in which the slow formation of an initial encounter complex is followed by ultra-fast zipping up of the encounter complex, to form a duplex. However, the $R_{2,ES}$ value from $R_{1\rho}$ experiment assuming $R_{2,GS} \neq R_{2,ES}$ is more reasonable (Table S3); the reason for this requires further investigation.

Calculation of hybridization kinetic parameters

The dissociation k_{off} (s^{-1}) and annealing k_{on} ($M^{-1}s^{-1}$) rate constants were determined based on the forward rate (k_1) and backward (k_{-1}) rates measured using the $R_{1\rho}$ and CEST experiments:

$$k_1 = k_{\mathrm{off}}$$

$$k_{-1} = k_{\mathrm{on}} \times [\mathrm{ss}]$$

$$[\mathrm{ss}] = \mathrm{C_T p_{ss}}$$

[ss] is the free concentration of the complementary single strand, p_{ss} is single strand population and C_T is the total concentration of the duplex. Since under slow exchange k_{-1} is ill defined by the $R_{1\rho}$ data, k_{-1} was either directly obtained from CEST or from fitting $R_{1\rho}$ data while fixing p_{ss} to be equal to that obtained from CEST.

$$k_{-1} = k_{\mathrm{ex}}(1 - \mathrm{p_{ss}})$$

The annealing rate constant k_{on} is given by:

$$k_{\mathrm{on}} = \frac{k_{\mathrm{ex}}(1 - \mathrm{p_{ss}})}{\mathrm{C_T p_{ss}}}$$

The uncertainties in C_T (assumed to be 20 %) and for p_{ss}, and k_{ex} obtained from the CEST fitting were propagated to estimate the uncertainty in k_{on}.

Optical melting experiments

Experiments

Optical melting experiments were conducted on a PerkinElmer Lambda 25 UV/VIS spectrometer with a RTP 6 Peltier Temperature Programmer and a PCB 1500 Water Peltier System. All DNA and RNA samples after buffer exchange were diluted to a concentration 3 μM with NMR buffer. At least three measurements were carried out for each DNA and RNA duplex using a sample volume of 400 μL in a Teflon-stoppered 1 cm path length quartz cell. The absorbance at 260 nm was monitored while the temperature was varied between 15°C and 95°C, at a ramp rate of 1.0 °C/min. All the thermodynamic parameters from UV melting experiments were fitted as described previously[4]. Errors in thermodynamic values were computed as standard deviation of triplicate melting measurements.

Data analysis

UV melting experiments were used to measure the thermodynamic parameters of duplex melting under the conditions used to carry out NMR experiments. The melting temperature (T_m) and standard enthalpy change ($\Delta H^{\ominus}$) of hybridization reaction were obtained by fitting the absorbance of optical melting experiment to equation (1) and (2) simultaneously[17],

$$\mathrm{Absorbance} = \varepsilon_{ss} \times p_{ss} + \varepsilon_{ds} \times (1 - p_{ss}) \quad (1)$$

$$p_{ss} = 1 - \frac{1 + 4e^{\left(\frac{1}{T_m} - \frac{1}{T}\right)\frac{\Delta H^{\ominus}}{R}} - \sqrt{1 + 8e^{\left(\frac{1}{T_m} - \frac{1}{T}\right)\frac{\Delta H^{\ominus}}{R}}}}{4e^{\left(\frac{1}{T_m} - \frac{1}{T}\right)\frac{\Delta H^{\ominus}}{R}}} \quad (2)$$

where ε_{ss} and ε_{ds} are molar extinction coefficients for the single and double strand, respectively, T is the temperature (K), *R* is the gas constant (kcal•mol^{-1}) and p_{ss} is the population of the single strand.

To account for differences between the concentrations used in UV and NMR, we computed the concentration dependent T_m using equation (3) adapted from the van't Hoff equation (4):

$$T_{m,2} = \frac{1}{\left(\frac{R}{\Delta H^{\Theta}}\left(\ln\left(\frac{C_{T,2}}{2}\right) - \ln\left(\frac{C_{T,1}}{2}\right)\right) + \frac{1}{T_{m,1}}\right)} \quad (3)$$

$$\ln\left(\frac{K_2^{\Theta}}{K_1^{\Theta}}\right) = \frac{-\Delta H^{\Theta}}{R}\left(\frac{1}{T_1} - \frac{1}{T_2}\right) \quad (4)$$

where $T_{m,1}$ and $T_{m,2}$ are melting temperature of double strand DNA or RNA with its concentrations. $C_{T,1}$ and $C_{T,2}$, respectively and R is the gas constant (kcal•mol^{-1}). K_1 and K_2 denote the equilibrium constant for melting. Standard entropy change (ΔS^{Θ}) and ΔG^{Θ} of double strand hybridization were therefore computed from equations (5) and (6):

$$\Delta S^{\Theta} = \frac{\Delta H^{\Theta}}{T_m} - R\ln\left(\frac{C_T}{2}\right) \quad (5)$$

$$\Delta G^{\Theta} = \Delta H^{\Theta} - T\Delta S^{\Theta} \quad (6)$$

The uncertainty in C_T was estimated to be 20% and the uncertainty in T_m and ΔH^{Θ} were obtained based on the standard deviation in triplicate measurement which were propagated to the uncertainty of ΔS^{Θ} and ΔG^{Θ}.

It should be noted that systematic differences (~ 1 kcal/mol) are observed between the $\Delta G^{\ominus}$ values measured using UV melting and NMR CEST experiments (Table S7). Because NMR experiments were preformed near T_m, small differences between the temperature in the NMR and UV instruments could lead to large differences in the measured p_{ss} and therefore $\Delta G^{\ominus}$ values. For example, for A_6-DNA, a difference in 3.0 °C can give rise to a difference of ~1.0 kcal/mol in $\Delta G^{\ominus}$. The difference could also arise from differences in oligonucleotide concentration caused by differential sample evaporation during UV and NMR as well as due to errors in the T_m extrapolation using the van't Hoff equation (4) due to deviations in the assumed temperature independence for $\Delta H^{\ominus}$ and $\Delta S^{\ominus}$. $\Delta G^{\ominus}$ and p_{ss} can in principle also be estimated from the integrated volumes of resonances in 2D HSQC spectra. However the volumes also depend on the longitudinal (R_1) and transverse (R_2) relaxation rates for double and single-stranded species as well as scalar couplings and delay times used in the HSQC experiment[18]. Despite these added complications, the $\Delta G^{\ominus}$ values measured by CEST and integrated volumes in 2D HSQC spectra are generally within ~0.8 kcal/mol.

Supplementary Figure

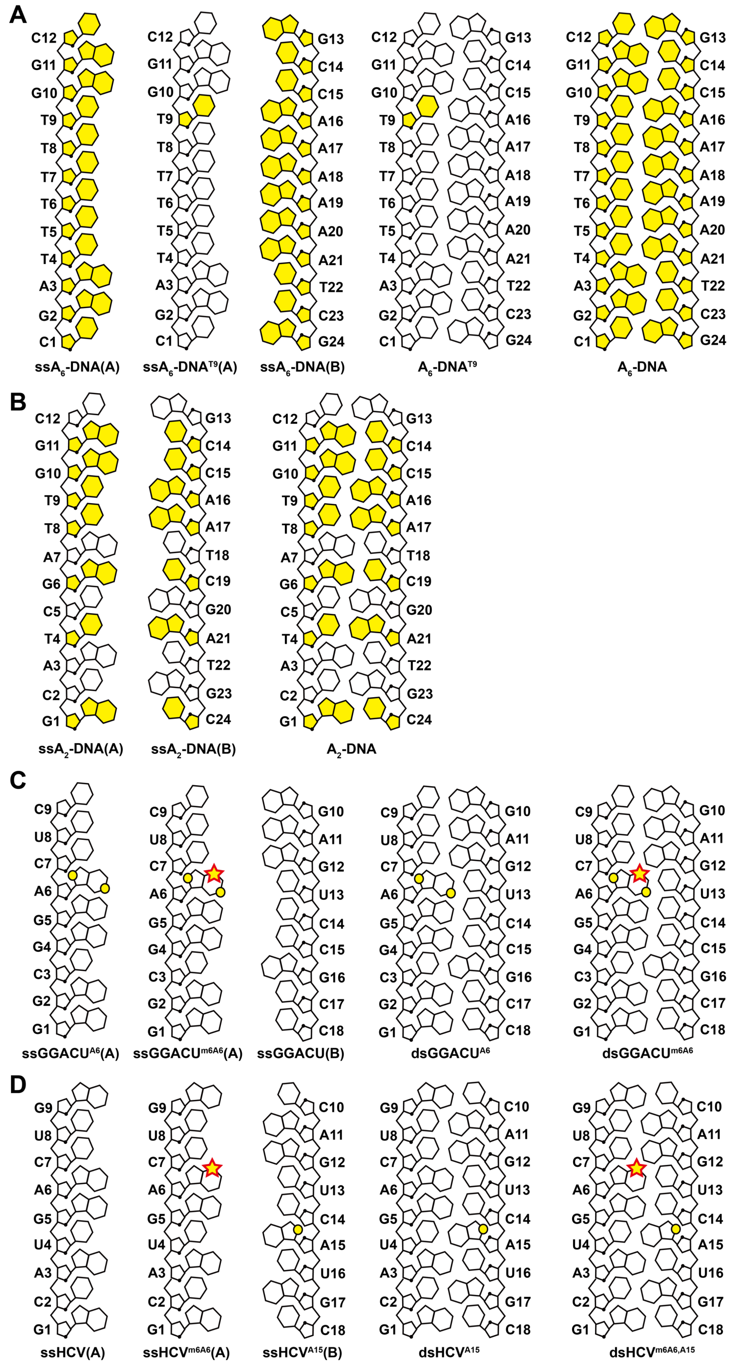

Figure S1. DNA and RNA oligonucleotides used in this study. (A) A_6-DNA **(B)** A_2-DNA **(C)** dsGGACU and **(D)** dsHCV RNA. $^{13}C/^{15}N$ Isotopically labeled nuclei are highlighted in yellow and m^6A is shown as a red star.

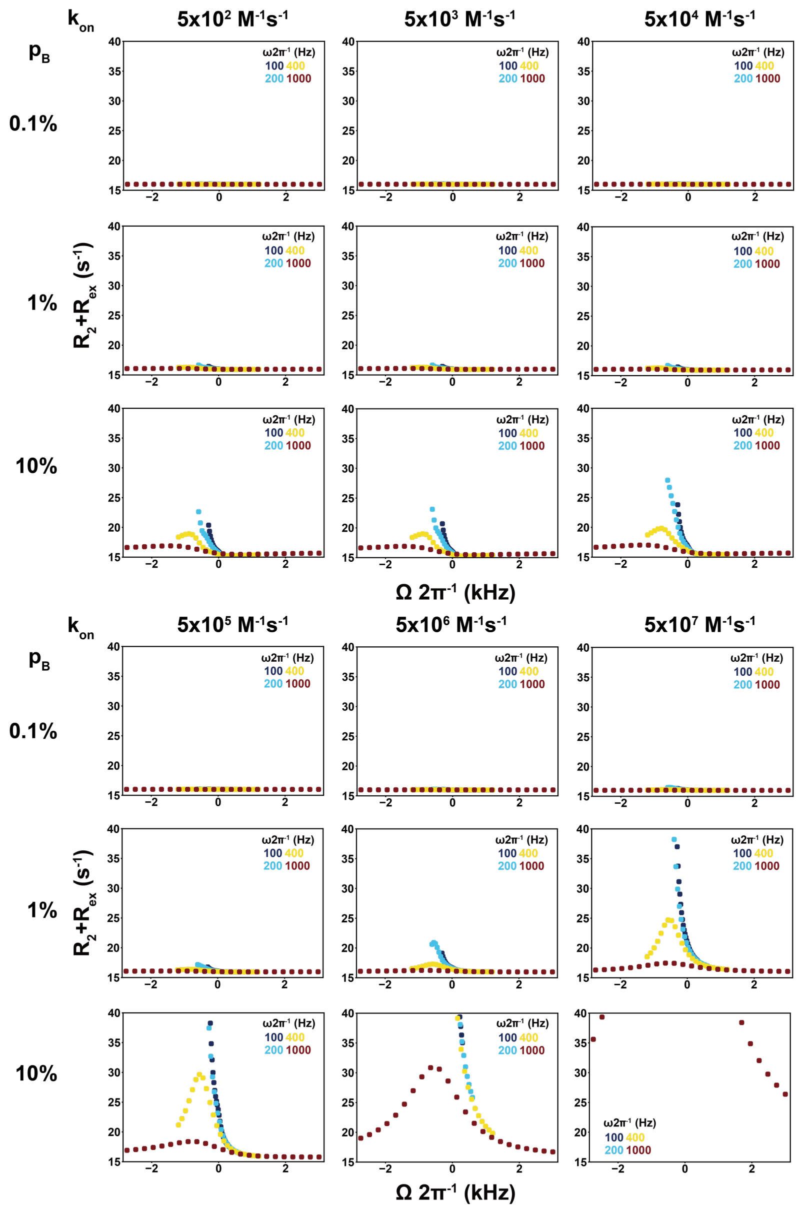

Figure S2. Bloch-McConnell simulations examining sensitivity of ^{13}C $R_{1\rho}$ RD to DNA duplex hybridization. Shown are a series of simulated $R_{1\rho}$ off-resonance profiles assuming k_{on} ranging between 5x10^2 and 5x10^7 M^{-1}s^{-1} [19] and p$_B$ ranging between 0.1% and 10% with R_1 = 2.5 s^{-1}, $R_{2,GS}$ = $R_{2,ES}$ = 16 s^{-1}, Δω = 3 ppm (B$_0$ = 700 MHz) and C$_T$ = 1 mM. Relaxation delay is 50 ms. Alignment of the effective field for the simulations was performed as described previously[11]. Spin-lock powers are color-coded.

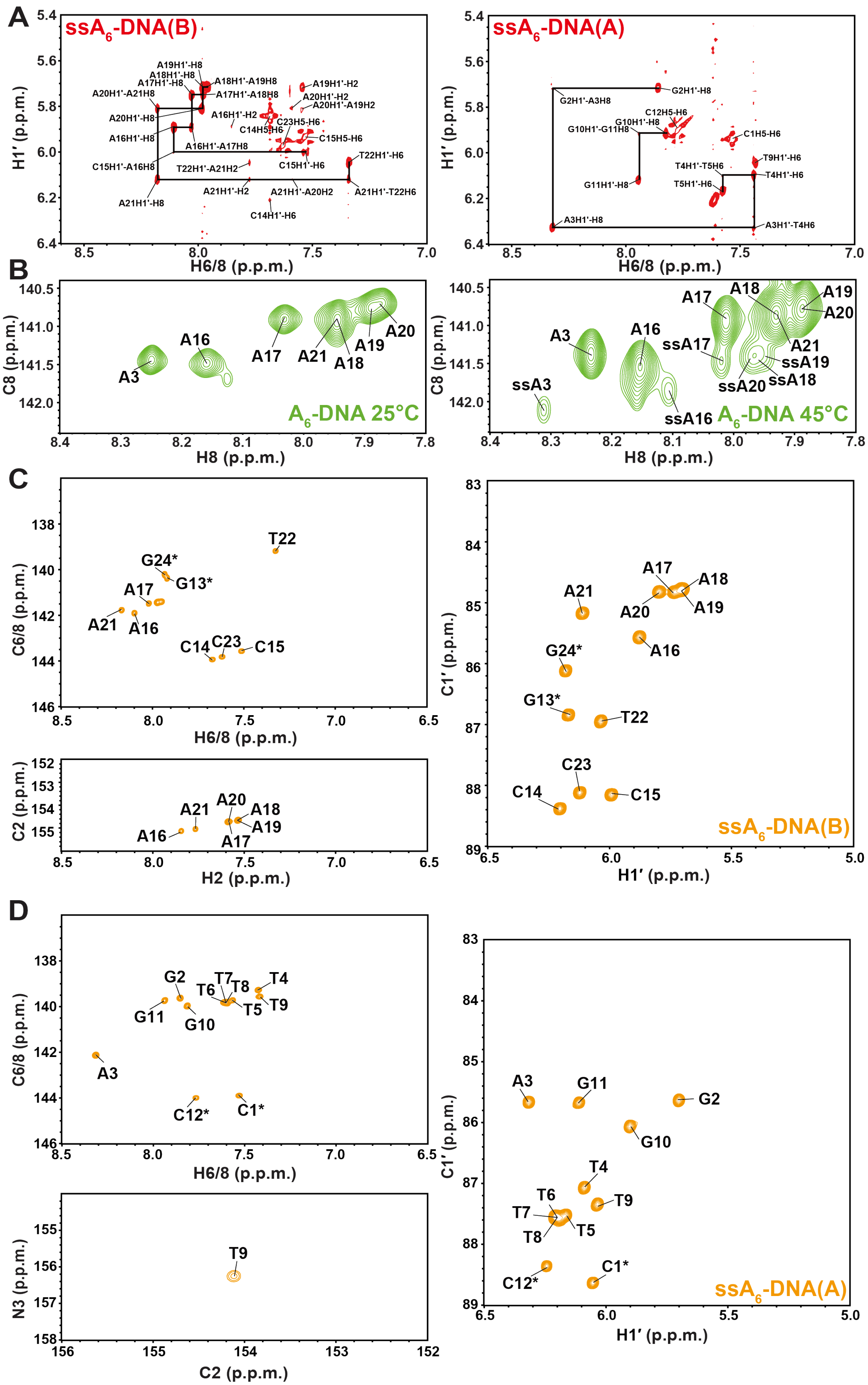
A
ssA6-DNA(B)
ssA6-DNA(A)
H1′ (p.p.m.)
H6/8 (p.p.m.)
B
A6-DNA 25°C
A6-DNA 45°C
C8 (p.p.m.)
H8 (p.p.m.)
C
C6/8 (p.p.m.)
C2 (p.p.m.)
H2 (p.p.m.)
C1′ (p.p.m.)
ssA6-DNA(B)
D
N3 (p.p.m.)
C2 (p.p.m.)
ssA6-DNA(A)

Figure S3. 2D [^{13}C, ^{1}H] and [^{15}N, ^{13}C] HSQC spectra of A_6-DNA and ssA_6-DNA showing the resonances targeted for RD measurements. **(A)** H1′-H8 region of the 2D [^{1}H, ^{1}H] NOESY spectra of ss-A_6DNA (A) and (B) with the H1′-H8 walk indicated using dashed lines (mixing time = 350 ms, at 45°C). **(B)** 2D [^{13}C, ^{1}H] HSQC spectra of the aromatic region of uniformly ^{13}C/^{15}N labeled A_6-DNA at 25°C and 45°C. The contour is lowered to such that ss peaks can be observed at 45°C. 2D [^{13}C, ^{1}H] and [^{15}N, ^{13}C] HSQC spectra of the aromatic and aliphatic regions of uniformly ^{13}C/^{15}N labeled **(C)** ssA_6-DNA(B) and **(D)** ssA_6-DNA(A) at 45°C. Star denotes sites for which the assignments were inferred from single stranded A_2-DNA.

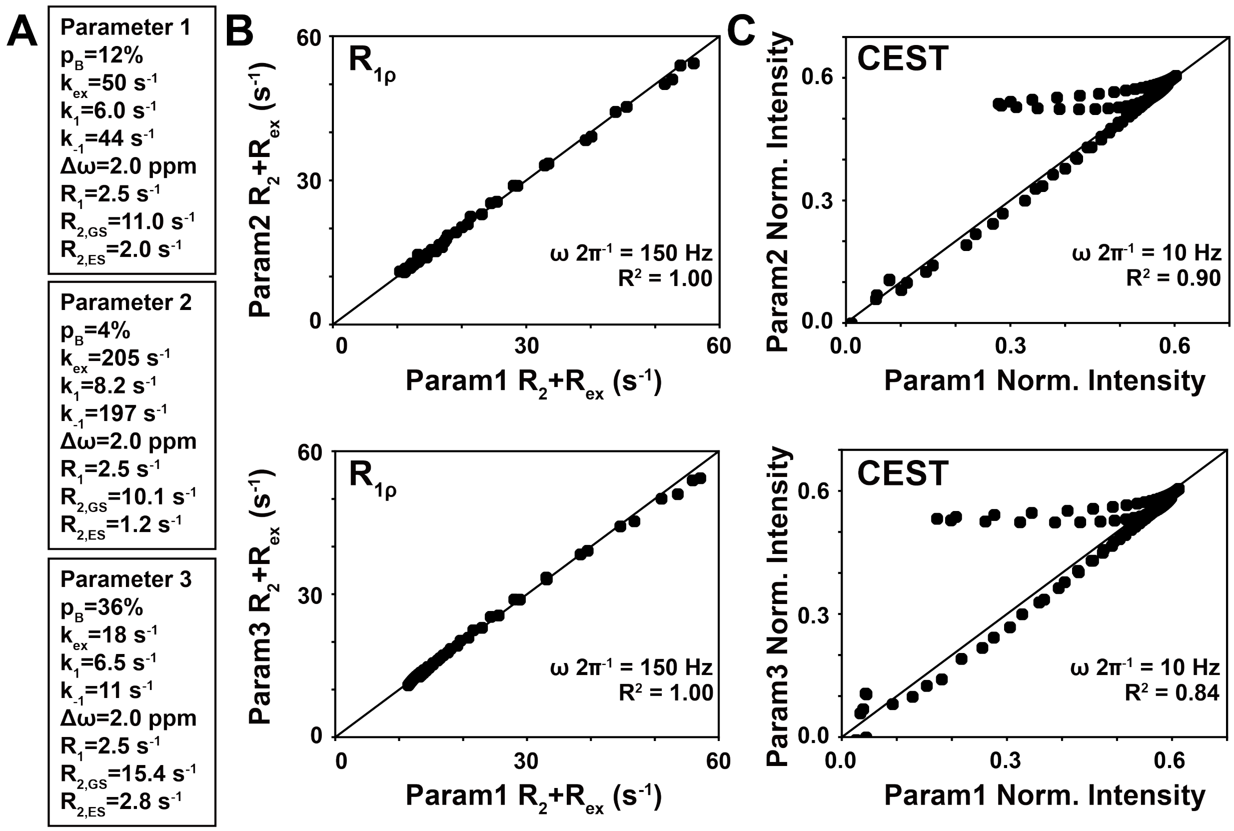

Figure S4. BM simulations to assess the k_{-1} degeneracy using $R_{1\rho}$ and CEST. (A) Three sets of exchange parameters used in the simulations (for B_0=700 MHz) with similar k_1 but varying k_{-1}. **(B, C)** Comparison of simulated **(B)** R_2+R_{ex} values for $R_{1\rho}$ and **(C)** normalized intensity values for CEST for the different exchange regimes. The spin-lock power is indicated in inset.

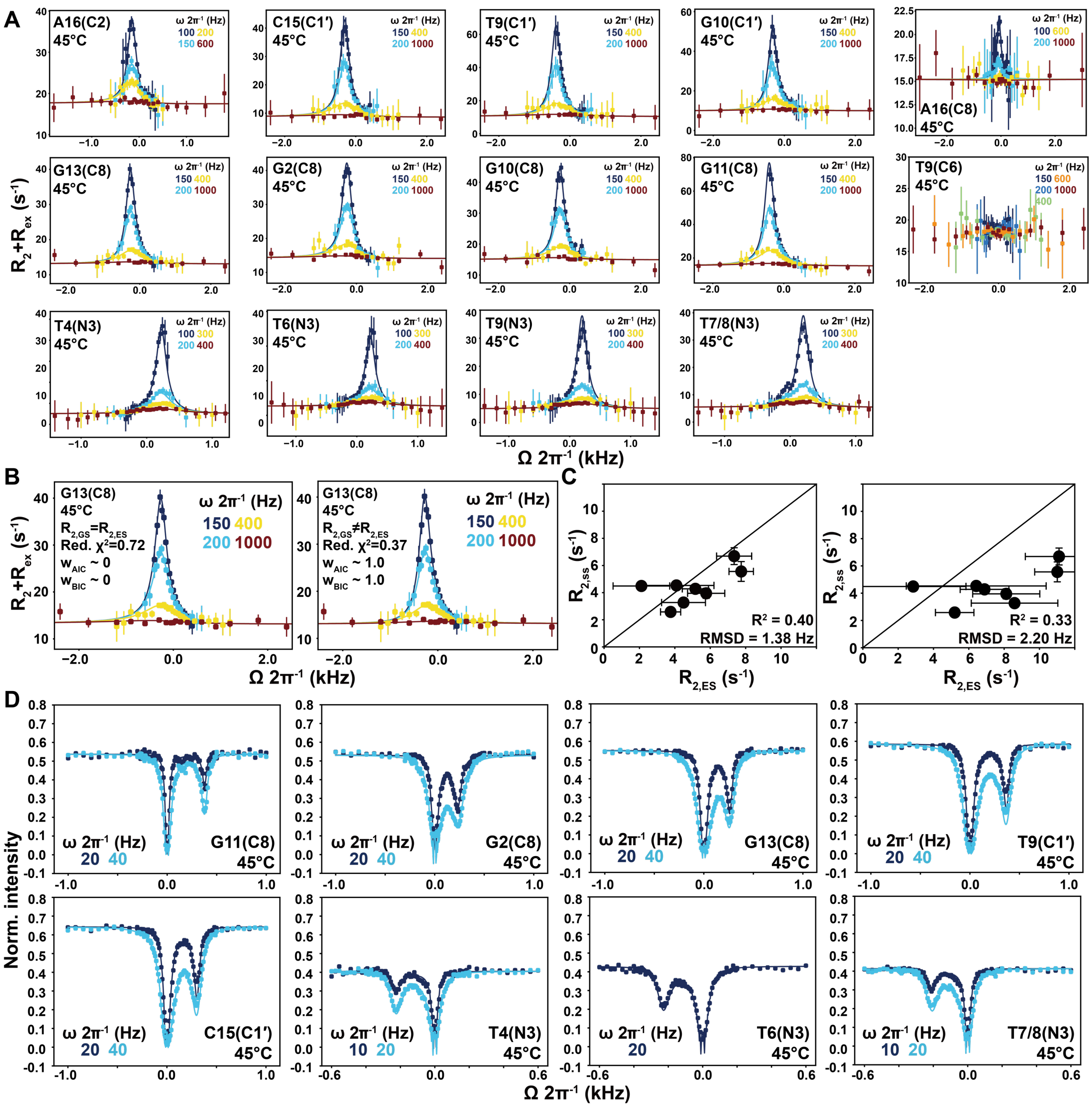

Figure S5. $^{13}C/^{15}N$ off-resonance $R_{1\rho}$ RD profiles and CEST profiles measured for A_6-DNA. Shown are **(A)** $^{13}C/^{15}N$ off-resonance $R_{1\rho}$ RD profiles measured for A_6-DNA at 45°C. Data is globally fitted assuming p_{ss} = 8.5% obtained from CEST experiments and with $R_{2,GS} \neq R_{2,GS}$. Spin-lock powers are color-coded. Errors were determined using Monte carlo scheme as described previously[12]. Alignment of the effective field for the simulations was performed as described previously[11]. **(B)** Comparison of $R_{1\rho}$ fitting of G13(C8) at 45°C with $R_{2,GS}=R_{2,ES}$ (left) and $R_{2,GS} \neq R_{2,ES}$ (right). Statistical Akaike's information criterion and Bayesian information criterion weights (w_{AIC} and w_{BIC}, respectively) comparing these two models are also shown. **(C)** Comparison of $R_{2,ES}$ measured by $R_{1\rho}$ RD with the values $R_{2,ss}$ measured directly from samples containing the two isolated ss. The left correlation plot is for p_{ss} = 15.6% estimated from UV melting while the right correlation plot is for p_{ss} = 8.5% estimated from CEST. **(D)** $^{13}C/^{15}N$ CEST measured for A_6-DNA at 45°C. Spin-lock powers are color-coded. Error bars denote experimental uncertainty as described in the Method Section.

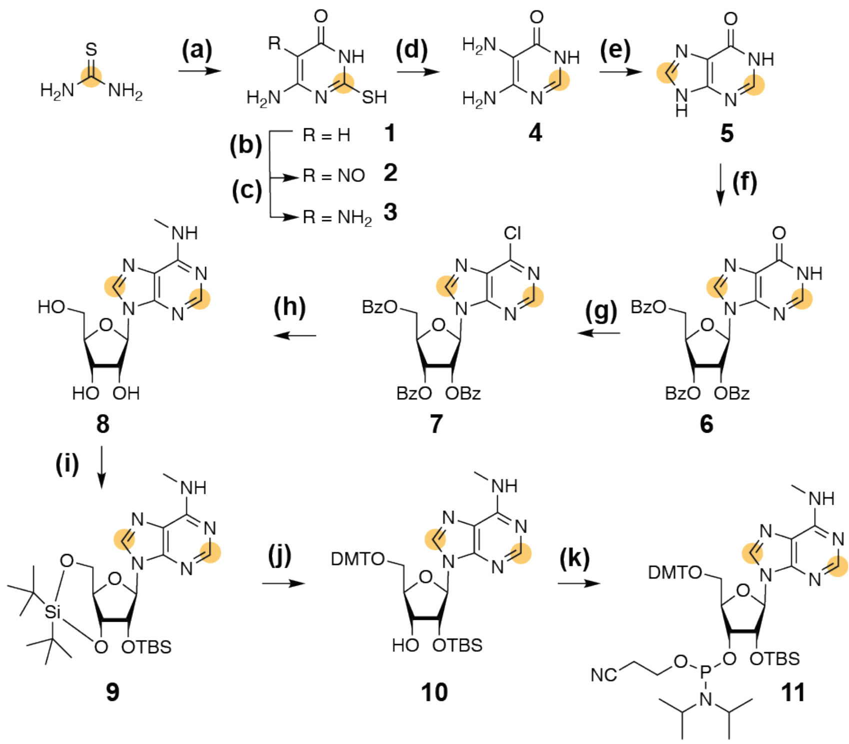

Figure S6. Synthesis of 2,8-$^{13}C_2$-6-CH_3-adenosine building block 11.

(a) ethyl cyanoactetate, sodium in absolute ethanol, 2h, 100°C, quantitative;

(b) sodium nitrite in 1M HCl, 3h, 0°C, quantitative;

(c) sodium dithionite in saturated sodium bicarbonate solution, 3h, 0°C, 94%;

(d) RaneyNi in 5% ammonia solution, 2h, 80°C, 82%;

(e) ^{13}C-formic acid, H_2SO_4 in H_2O, 3h, 100°C, 65%;

(f) 1-*O*-acetyl-(2′,3′,5′-*O*-tri-benzoyl)-*β*-*D*-ribofuranose (ATBR), bis-(trimethylsilyl)-acetamide (BSA), trimethylsilyltrifluoro-methane sulfonate (TMSOTf) in xylene, 1h, 100 °C, 72 %;

(g) SO_2Cl_2 in $CHCl_3$, 3h, reflux, 62%;

(h) CH_3NH_2 in ethanol (33 wt%), CH_3NH_2 in H_2O (40 wt%), 48h, rt, 90%;

(i) *t*-$Bu_2Si(OTf)_2$ in DMF, 0°C, 1h, then *t*-$BuMe_2SiCl$, imidazole in DMF, 60°C, 2h, 67%;

(j) HF.Py in CH_2Cl_2, 0°C, 2h, then DMT-Cl in pyridine, rt, 3h, 61%;

(k) 2-cyanoethyl-N,N-diisopropylchlorophosphoramidite, DiPEA in THF, 3h, rt, 61%.

Orange dot = ^{13}C.

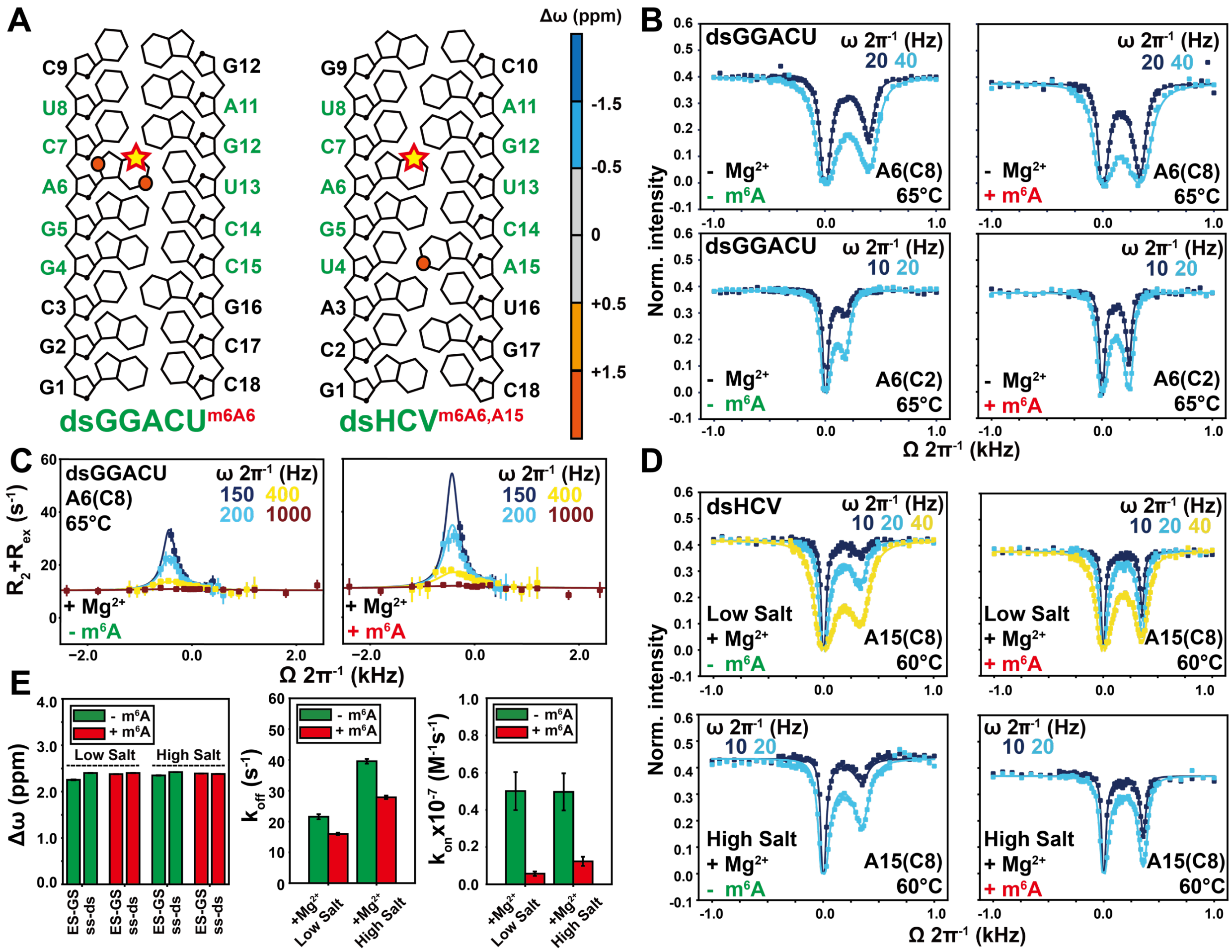

Figure S7. Additional datasets characterizing RNA hybridization kinetics using NMR CEST and $R_{1\rho}$ RD. (A) The dsGGACU and dsHCV sequences with m^{6}A denoted using a star and the DRACH consensus sequence highlighted in green. $\Delta\omega = \omega_{ES} - \omega_{GS}$ obtained from global fitting of CEST data is color-coded on each atom. **(B)** CEST and **(C)** $R_{1\rho}$ RD profiles measured at 65°C in the presence of Mg^{2+} for dsGGACU without (left, green) and with (right, red) m^{6}A. $R_{1\rho}$ data is fitted assuming p_{ss} from CEST with $R_{2,GS} \neq R_{2,ES}$. Errors were determined using Monte Carlo scheme as described previously[12]. Alignment of the effective field for the simulations was performed as described previously[11]. **(D)** CEST profiles measured in dsHCV without (left, green) and with (right, red) m^{6}A at 60°C and in the presence of Mg^{2+}at low salt (25mM NaCl, upper) and at high salt (100mM NaCl, lower). **(E)** Comparison of $\Delta\omega$, k_{on} and k_{off} measured for unmodified (green) and m^{6}A modified (red) for dsHCV. Error bars denote experimental uncertainty obtained from fitting CEST profiles, as described in Method Section. Spin-lock powers for $R_{1\rho}$ and CEST are color-coded.

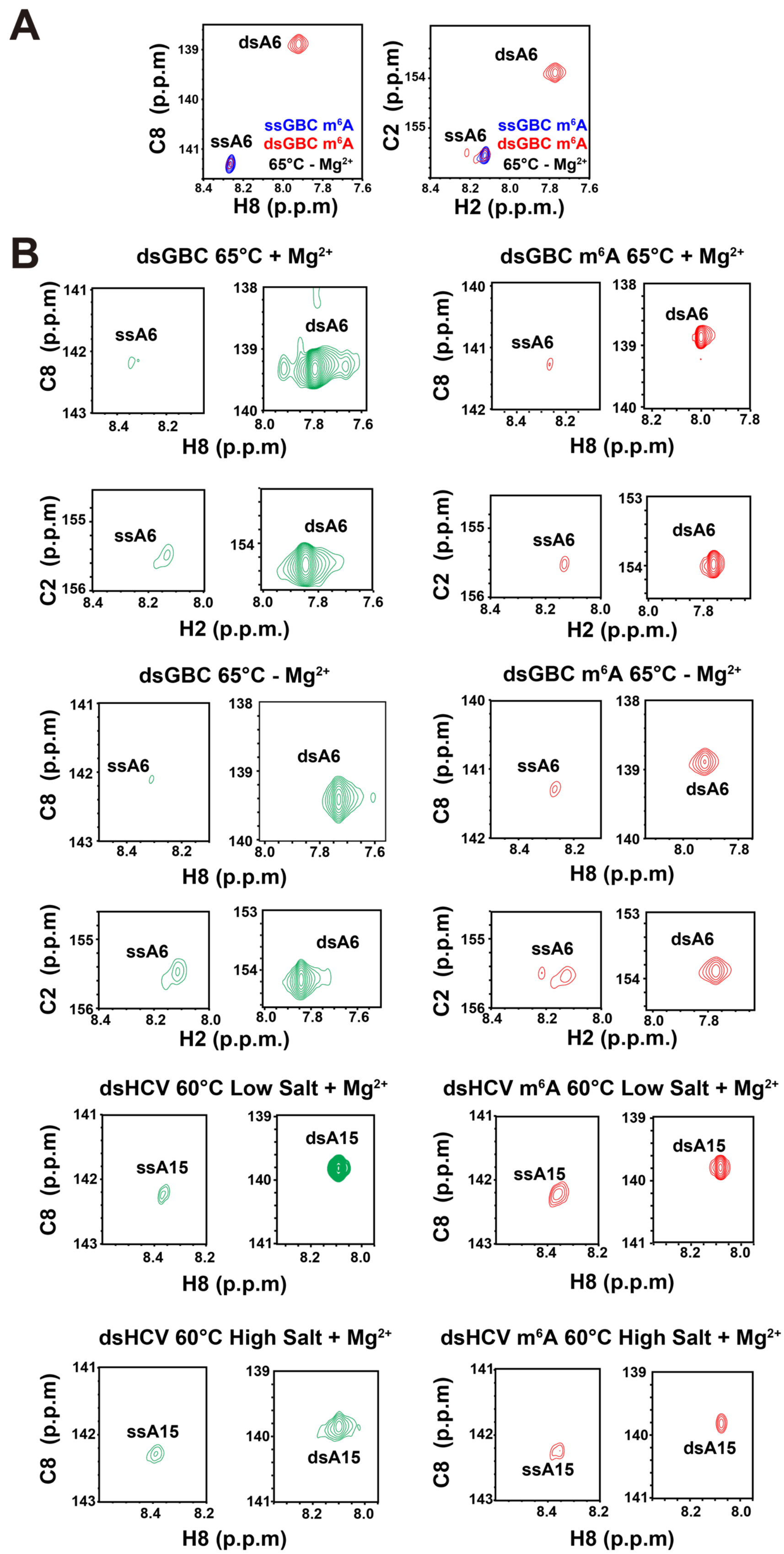
A
dsA6
ssA6
ssGBC m6A
dsGBC m6A
65°C - Mg2+
C8 (p.p.m)
H8 (p.p.m)
C2 (p.p.m)
H2 (p.p.m.)
B
dsGBC 65°C + Mg2+
dsGBC m6A 65°C + Mg2+
dsGBC 65°C - Mg2+
dsGBC m6A 65°C - Mg2+
dsHCV 60°C Low Salt + Mg2+
dsHCV m6A 60°C Low Salt + Mg2+
dsHCV 60°C High Salt + Mg2+
dsHCV m6A 60°C High Salt + Mg2+
ssA15
dsA15

Figure S8. 2D [^{13}C,^{1}H] HSQC spectra of site labeled ssGGACU^{m6A6}(A), dsGGACU^{A6}, dsGGACU^{m6A6} , dsHCV^{A15} and dsHCV^{m6A6,A15}, showing the resonances targeted for RD measurements. **(A)** 2D [^{13}C,^{1}H] HSQC spectra overlay of site labeled ssGGACU^{m6A6}(A) and dsGGACU^{m6A6} at 65°C in the absence of Mg^{2+}. **(B)** 2D [^{13}C,^{1}H] HSQC spectra of site labeled dsGGACU^{A6}, dsGGACU^{m6A6} at 65°C in the presence and absence of Mg^{2+}, and of site labeled dsHCV^{A15} and dsHCV^{m6A6,A15} at 60°C in the presence of Mg^{2+} at low salt (25 mM NaCl) and high salt (100 mM NaCl) condition. Peaks representing ssRNA and dsRNA are shown.

Supplementary Tables

Supplementary Table 1. Duplex thermodynamic parameters from UV melting experiments. Shown are number of replicates (n), the Mg^{2+} (Mg^{2+}) and oligo concentration (Ct), melting temperature (T_m), standard enthalpy difference (ΔH^{Θ}), entropy difference (ΔS^{Θ}), and free energy difference for duplex melting at 25°C ($\Delta G^{\Theta}_{25°C}$).

Construct	n	Mg^{2+} (μM)	Ct (μM)	T_m(°C)	ΔH^{Θ} (kcal/mol)	ΔS^{Θ} (e.u.)	$\Delta G^{\Theta}_{25°C}$ (kcal/mol)
A_6-DNA	3	0	3	39.2±0.2	-98.6±2.9	-288.8±9.1	-12.5±0.2
A_2-DNA	3	0	3	47.4±0.2	-95.6±2.6	-271.7±7.9	-14.6±0.2
dsGGACU [(a)]	3	0	3	54.6±0.2	-86.1±1.5	-236.1±4.7	-15.7±0.1
$dsGGACU^{m6A6}$ [(a)]	3	0	3	51.2±0.2	-87.7±1.3	-243.7±4.0	-15.0±0.1
dsGGACU [(a)]	3	3	3	66.0±0.4	-94.9±1.1	-253.2±3.0	-16.4±0.2
$dsGGACU^{m6A6}$ [(a)]	3	3	3	63.4±0.1	-95.5±2.2	-257.0±6.6	-15.8±0.2
dsHCV	3	3	3	54.2±0.1	-107.5±0.5	-301.7±1.5	-17.5±0.1
$dsHCV^{m6A6}$	3	3	3	52.2±0.4	-104.4±0.2	-294.2±0.3	-16.7±0.1

Errors represent one s.d. (n=3 independent measurements). Uncertainty in the calculated thermodynamic parameters were determined by error propagation as described previously[20]. (a) Data from[21].

Supplementary Table 2. ***R_2*** **values measured for single stranded ssA$_6$-DNA(A) and ssA$_6$-DNA(B).**

Sample	Resonance	*R_2* (s^{-1})
ssA$_6$-DNA(A)	G2(C8)	5.56±0.73
	T9(C1′)	4.53±0.21
	G10(C1′)	4.49±0.02
	G10(C8)	4.28±0.21
	G11(C8)	3.95±0.37
ssA$_6$-DNA(B)	G13(C8)	2.58±0.13
	C15(C1′)	3.27±0.31
	A16(C2)	6.69±0.62

Supplementary Table 3. Exchange parameters from globally fitting ^{13}C and ^{15}N $R_{1\rho}$ data assuming p_{ss} derived from CEST. Shown is the chemical shift difference between GS and ES ($\Delta\omega$), single strand population (p_{ss}), exchange rate (k_{ex}), longitudinal relaxation rate (R_1), and transverse relaxation rate for the GS ($R_{2,GS}$) and ES ($R_{2,ES}$), and the reduced χ^2 for the fit.

Sample	Resonance	$\Delta\omega$ (ppm)	p_{ss} (%)	k_{ex} (s^{-1})	R_1 (s^{-1})	$R_{2,GS}$ (s^{-1})	$R_{2,ES}$ (s^{-1})	Red. χ^2
A_6-DNA 45°C	A16(C8)	0.50±0.01	8.5	84±1	2.80±0.06	16.41±0.27	2.38±2.36	0.48
	A16(C2)	0.89±0.01			3.22±0.06	18.15±0.17	11.11±1.91	
	G2(C8)	1.58±0.02			3.13±0.05	14.47±0.09	11.01±1.28	
	G10(C8)	1.61±0.02			2.98±0.06	15.70±0.11	6.89±1.38	
	G11(C8)	2.34±0.03			3.27±0.08	16.00±0.13	8.12±1.90	
	G13(C8)	1.54±0.01			3.23±0.04	13.83±0.09	5.20±1.09	
	T9(C1′)	2.23±0.06			2.35±0.16	10.84±0.25	6.42±3.96	
	C15(C1′)	1.77±0.03			1.91±0.09	8.70±0.16	8.59±2.45	
	G10(C1′)	1.93±0.04			2.45±0.14	10.57±0.21	2.85±2.99	
	T4(N3)	-3.20±0.05			2.70±0.07	5.20±0.14	3.24±1.95	
	T6(N3)	-3.20±0.08			2.60±0.11	5.59±0.21	2.07±2.99	
	T9(N3)	-2.92±0.04			2.73±0.07	5.02±0.13	2.80±1.78	
	T7/8(N3)	-2.93±0.03			2.67±0.05	5.86±0.10	0.00±1.26	
$dsGGACU^{A6}$, 65°C	A6(C8)	2.91±0.05	1.8	144±4	5.01±0.04	10.52±0.07	0.00±5.15	0.23
$dsGGACU^{m6A6}$, 65°C	A6(C8)	2.91±0.06	6.8	63±2	5.61±0.08	11.56±0.15	3.69±2.30	0.44

Supplementary Table 4. Exchange parameters from fitting ^{13}C and ^{15}N CEST data. Shown is the chemical shift difference between GS and ES (Δω), single strand population (p_{ss}), exchange rate (k_{ex}), longitudinal relaxation rate (R_1), the transverse relaxation rate for the GS ($R_{2,GS}$) and ES ($R_{2,ES}$), and the reduced χ^2 for the fit.

Sample	Resonance	Δω (ppm)	p_{ss} (%)	k_{ex} (s^{-1})	R_1 (s^{-1})	$R_{2,GS}$ (s^{-1})	$R_{2,ES}$ (s^{-1})	Red. χ^2
A_6-DNA 45°C	G11(C8)	2.15±0.00	8.5±0.1	93±1	2.66±0.00	13.21±0.07	28.63±0.92	26.8
	G2(C8)	1.34±0.00			2.71±0.00	4.75±0.05	85.48±1.14	
	G13(C8)	1.50±0.00			2.53±0.01	11.66±0.12	19.61±1.76	
	T9(C1′)	2.10±0.00			2.23±0.01	10.27±0.13	29.97±2.34	
	C15(C1′)	1.73±0.00			1.76±0.01	7.73±0.10	26.93±1.79	
	T4(N3)	-3.20±0.02			4.07±0.02	6.72±0.37	63.32±10.81	
	T6(N3)	-3.24±0.03			3.77±0.04	7.77±0.64	74.39±34.44	
	T7/8(N3)	-2.96±0.00			3.97±0.00	7.66±0.08	77.33±2.94	
A_6-DNA 50°C	G11(C8)	2.15±0.00	20.9±0.1	287±2	2.29±0.01	6.89±0.49	42.61±2.55	14.1
A_2-DNA 50°C	G11(C8)	2.14±0.00	5.1±0.1	57±1	3.42±0.00	13.46±0.04	36.38±1.04	96.5
$dsGGACU^{A6}$ no Mg^{2+}, 65°C	A6(C8)	2.65±0.00	9.2±0.0	291±2	4.14±0.00	7.68±0.10	68.26±1.71	7.5
	A6(C2)	1.28±0.00			4.30±0.00	9.30±0.23	32.05±5.77	
$dsGGACU^{m6A6}$ no Mg^{2+}, 65°C	A6(C8)	2.23±0.00	24.9±0.2	144±3	3.45±0.02	4.42±0.78	82.87±4.60	3.3
	A6(C2)	1.65±0.00			3.46±0.02	7.56±0.64	14.07±2.86	
$dsGGACU^{A6}$ Mg^{2+}, 65°C	A6(C8)	2.61±0.00	1.8±0.0	221±6	4.62±0.00	9.31±0.07	208.50±11.14	6.5
	A6(C2)	1.07±0.00			4.77±0.00	10.25±0.06	67.24±6.12	
$dsGGACU^{m6A6}$ Mg^{2+}, 65°C	A6(C8)	2.06±0.00	6.8±0.1	104±2	4.51±0.01	9.58±0.09	227.29±3.64	4.5
	A6(C2)	1.50±0.00			4.67±0.01	14.98±0.13	65.41±2.43	
$dsHCV^{A15}$ Mg^{2+}, 60°C	A15(C8)	2.25±0.01	7.5±0.1	286±10	3.99±0.01	9.90±0.56	136.37±11.83	2.5
$dsHCV^{m6A6,A15}$ Mg^{2+}, 60°C	A15(C8)	2.38±0.00	18.1±0.0	88±2	3.88±0.01	6.30±0.24	23.00±1.50	6.4
$dsHCV^{A15}$ Mg^{2+}, 60°C [(a)]	A15(C8)	2.35±0.00	13.2±0.1	301±5	3.48±0.01	0.00±0.00	165.67±10.06	13.0
$dsHCV^{A15}$ Mg^{2+}, 60°C [(a)]	A15(C8)	2.39±0.00	21.1±0.2	132±2	3.79±0.01	0.00±0.00	36.70±2.51	10.7

(a) [NaCl] = 100 mM

Supplementary Table 5. Spin-lock power and offsets used in the $R_{1\rho}$ measurements.

Nuclei	[spin-lock power] {offset frequencies}
	[ω_1 $2\pi^{-1}$(s^{-1})] {Ω $2\pi^{-1}$(s^{-1})}
A_6-DNA, 25°C, Bruker 700 MHz	
A16(C2)	[150, 200, 250, 300, 400, 500, 600, 700, 900, 1000, 1200, 1400, 1600, 2000, 2500] {0} [150] {-400, -340, -280, -240, -200, -160, -120, -80, -40, 40, 80, 120, 160, 200, 240, 280, 340, 400} [200] {-600, -500, -400, -350, -300, -250, -200, -150, -100, -50, 50, 100, 150, 200, 250, 300, 350, 400, 500, 600} [400] {-1200, -1050, -900, -750, -600, -450, -300, -250, -200, -150, -100, -50, 50, 100, 150, 200, 250, 300, 450, 600, 750, 900, 1050, 1200} [1000] {-2400, -1800, -1200, -900, -600, -300, -150, -50, 50, 150, 300, 600, 900, 1200, 1800, 2400}
A16(C8)	[150, 200, 250, 300, 400, 500, 600, 700, 900, 1000, 1200, 1400, 1600, 2000, 2500] {0} [200] {-600, -500, -450, -400, -400, -350, -300, -250, -200, -150, -100, -50, 100, 200, 400} [400] {-1000, -850, -700, -650, -600, -550, -500, -450, -400, -400, -350, -300, -250, -200, -150, -100, 50, 200, 350, 500, 650, 800, 1000, 1200} [600] {-1400, -1200, -1000, -800, -700, -600, -550, -500, -450, -400, -400, -350, -300, -250, -200, -100, 200, 400, 600, 1000, 1400, 1800} [1000] {-2200, -1600, -1300, -1000, -700, -550, -450, -400, -400, -350, -250, -100, 200, 500, 800, 1400, 2000}
A_6-DNA, 45°C, Bruker 700 MHz	
A16(C2)	[100, 150, 200, 250, 300, 400, 500, 600, 700, 900, 1000, 1200, 1400, 1600, 2000, 2500] {0} [100] {-340, -280, -240, -200, -160, -120, -80, -40, 40, 80, 120, 160, 200, 240, 280, 340} [150] {-500, -340, -280, -240, -200, -160, -120, -80, -40, 40, 80, 120, 160, 200, 240, 280, 340, 400, 500} [200] {-600, -500, -400, -350, -300, -250, -200, -150, -100, -50, 50, 100, 150, 200, 250, 300, 350, 400, 500} [600] {-1800, -1400, -1000, -800, -600, -400, -300, -200, -150, -100, -50, 50, 100, 150, 200, 300, 400, 600, 800, 1000, 1400, 1800}
A16(C8)	[100, 150, 200, 250, 300, 400, 500, 600, 700, 900, 1000, 1200, 1400, 1600, 2000, 2500] {0} [100] {-340, -280, -240, -200, -160, -120, -80, -40, 40, 80, 120, 160, 200, 240, 280, 340} [200] {-600, -500, -400, -350, -300, -250, -200, -150, -100, -50, 50, 100, 150, 200, 250, 300, 350, 400, 500, 600} [600] {-1400, -1000, -800, -600, -400, -300, -200, -150, -100, -50, 50, 100, 150, 200, 300, 400, 600, 800, 1000, 1400} [1000] {-3000, -2400, -1800, -1200, -900, -600, -300, -150, -50, 50, 150, 300, 600, 900, 1200, 1800, 3000}
C15(C1′)	[150, 200, 250, 300, 400, 500, 600, 700, 900, 1000, 1200, 1400, 1600, 2000, 2500] {0} [150] {-400, -340, -280, -240, -200, -160, -120, -80, -40, 40, 80, 120, 160, 200, 240, 280, 340, 400} [200] {-600, -500, -400, -350, -300, -250, -200, -150, -100, -50, 50, 100, 150, 200, 250, 300, 350, 400, 500, 600}

	[400] {-1200, -1050, -900, -750, -600, -450, -300, -250, -200, -150, -100, -50, 50, 100, 150, 200, 250, 300, 450, 600, 750, 900, 1050, 1200} [1000] {-2400, -1800, -1200, -900, -600, -300, -150, -50, 50, 150, 300, 600, 900, 1200, 1800, 2400}
G10(C1′)	[150, 200, 250, 300, 400, 500, 600, 700, 900, 1000, 1200, 1400, 1600, 2000, 2500] {0} [150] {-400, -340, -280, -240, -200, -160, -120, -80, -40, 40, 80, 120, 160, 200, 240, 280, 340, 400} [200] {-600, -500, -400, -350, -300, -250, -200, -150, -100, -50, 50, 100, 150, 200, 250, 300, 350, 400, 500, 600} [400] {-1200, -1050, -900, -750, -600, -450, -300, -250, -200, -150, -100, -50, 50, 100, 150, 200, 250, 300, 450, 600, 750, 900, 1050, 1200} [1000] {-2400, -1800, -1200, -900, -600, -300, -150, -50, 50, 150, 300, 600, 900, 1200, 1800, 2400}
G10(C8)	[150, 200, 250, 300, 400, 500, 700, 900, 1000, 1200, 1400, 1600, 2000, 2500] {0} [150] {-400, -340, -280, -240, -200, -160, -120, -80, -40, 40, 80, 120, 160, 200, 240, 280, 340} [200] {-600, -500, -400, -350, -300, -250, -200, -150, -100, -50, 50, 100, 150, 200, 250, 300, 350, 400} [400] {-1200, -1050, -900, -750, -600, -450, -300, -250, -200, -150, -100, -50, 50, 100, 150, 200, 250, 300, 450, 600, 750, 1050, 1200} [1000] {-2400, -1800, -1200, -900, -600, -300, -150, -50, 50, 150, 300, 600, 900, 1200, 1800, 2400}
G11(C8)	[150, 200, 250, 300, 400, 500, 600, 700, 900, 1000, 1200, 1400, 1600, 2000, 2500] {0} [150] {-400, -340, -280, -240, -200, -160, -120, -80, -40, 40, 80, 120, 160, 200, 240, 280, 340, 400} [200] {-600, -500, -400, -350, -300, -250, -200, -150, -100, -50, 50, 100, 150, 200, 250, 300, 350, 400, 500, 600} [400] {-1200, -1050, -900, -750, -600, -450, -300, -250, -200, -150, -100, -50, 50, 100, 150, 200, 250, 300, 450, 600, 750, 900, 1050, 1200} [1000] {-2400, -1800, -1200, -900, -600, -300, -150, -50, 50, 150, 300, 600, 900, 1200, 1800, 2400}
G13(C8)	[150, 200, 250, 300, 400, 500, 600, 700, 900, 1000, 1200, 1400, 1600, 2000, 2500] {0} [150] {-400, -340, -280, -240, -200, -160, -120, -80, -40, 40, 80, 120, 160, 200, 240, 280, 340, 400} [200] {-600, -500, -400, -350, -300, -250, -200, -150, -100, -50, 50, 100, 150, 200, 250, 300, 350, 400, 500, 600} [400] {-1200, -1050, -900, -750, -600, -450, -300, -250, -200, -150, -100, -50, 50, 100, 150, 200, 250, 300, 450, 600, 750, 900, 1050, 1200} [1000] {-2400, -1800, -1200, -900, -600, -300, -150, -50, 50, 150, 300, 600, 900, 1200, 1800, 2400}
G2(C8)	[150, 200, 250, 300, 400, 500, 600, 700, 900, 1000, 1200, 1400, 1600, 2000, 2500] {0} [150] {-400, -340, -280, -240, -200, -160, -120, -80, -40, 40, 80, 120, 160, 200, 240, 280, 340, 400} [200] {-600, -500, -400, -350, -300, -250, -200, -150, -100, -50, 50, 100, 150, 200, 250, 300, 350, 400, 500, 600} [400] {-1200, -1050, -900, -750, -600, -450, -300, -250, -200, -150, -100, -50, 50, 100, 150, 200, 250, 300, 450, 600, 750, 900, 1050, 1200} [1000] {-2400, -1800, -1200, -900, -600, -300, -150, -50, 50, 150, 300, 600, 900, 1200, 1800, 2400}

T4(N3)	[50, 100, 150, 200, 250, 300, 400, 500, 600, 700, 900, 1000, 1200, 1400, 1600, 2000, 2500] {0} [100] {-320, -280, -240, -210, -180, -150, -120, -90, -60, -30, 30, 60, 90, 120, 150, 180, 210, 240, 280, 320} [200] {-600, -500, -400, -350, -300, -250, -200, -150, -100, -50, 50, 100, 150, 200, 250, 300, 350, 400, 500, 600} [300] {-1000, -800, -600, -500, -400, -350, -300, -250, -200, -150, -100, -50, 50, 100, 150, 200, 250, 300, 350, 400, 500, 600, 800, 1000} [400] {-1400, -1200, -1050, -900, -750, -600, -450, -300, -250, -200, -150, -100, -50, 50, 100, 150, 200, 250, 300, 450, 600, 750, 900, 1050, 1200}
T6(N3)	[50, 100, 150, 200, 250, 300, 400, 500, 600, 700, 900, 1000, 1200, 1400, 1600, 2000, 2500] {0} [100] {-320, -280, -240, -210, -180, -150, -120, -90, -60, -30, 30, 60, 90, 120, 150, 180, 210, 240, 280, 320} [200] {-600, -500, -400, -350, -300, -250, -200, -150, -100, -50, 50, 100, 150, 200, 250, 300, 350, 400, 500, 600} [300] {-1000, -800, -600, -500, -400, -350, -300, -250, -200, -150, -100, -50, 50, 100, 150, 200, 250, 300, 350, 400, 500, 600, 800, 1000} [400] {-1400, -1200, -1050, -900, -750, -600, -450, -300, -250, -200, -150, -100, -50, 50, 100, 150, 200, 250, 300, 450, 600, 750, 900, 1050, 1200, 1400}
T78(N3)	[50, 100, 150, 200, 250, 300, 400, 500, 600, 700, 900, 1000, 1200, 1400, 1600, 2000, 2500] {0} [100] {-320, -280, -240, -210, -180, -150, -120, -90, -60, -30, 30, 60, 90, 120, 150, 180, 210, 240, 280, 320} [200] {-600, -500, -400, -350, -300, -250, -200, -150, -100, -50, 50, 100, 150, 200, 250, 300, 350, 400, 500, 600} [300] {-1000, -800, -600, -500, -400, -350, -300, -250, -200, -150, -100, -50, 50, 100, 150, 200, 250, 300, 350, 400, 500, 600, 800, 1000} [400] {-1400, -1200, -1050, -900, -750, -600, -450, -300, -250, -200, -150, -100, -50, 50, 100, 150, 200, 250, 300, 450, 600, 750, 900, 1050, 1200}
T9(C1′)	[150, 200, 250, 300, 400, 500, 600, 700, 900, 1000, 1200, 1400, 1600, 2000, 2500] {0} [150] {-400, -340, -280, -240, -200, -160, -120, -80, -40, 40, 80, 120, 160, 200, 240, 280, 340, 400} [200] {-600, -500, -400, -350, -300, -250, -200, -150, -100, -50, 50, 100, 150, 200, 250, 300, 350, 400, 500, 600} [400] {-1200, -1050, -900, -750, -600, -450, -300, -250, -200, -150, -100, -50, 50, 100, 150, 200, 250, 300, 450, 600, 750, 900, 1050, 1200} [1000] {-2400, -1800, -1200, -900, -600, -300, -150, -50, 50, 150, 300, 600, 900, 1200, 1800, 2400}
T9(C6)	[150, 200, 250, 300, 400, 500, 600, 700, 900, 1000, 1200, 1400, 1600, 2000, 2500] {0} [150] {-400, -340, -280, -240, -200, -160, -120, -80, -40, 40, 80, 120, 160, 200, 240, 280, 340, 400} [200] {-600, -500, -400, -350, -300, -250, -200, -150, -100, -50, 50, 100, 150, 200, 250, 300, 350, 400, 500, 600} [400] {-1200, -1050, -900, -750, -600, -450, -300, -250, -200, -150, -100, -50, 50, 100, 150, 200, 250, 300, 450, 600, 750, 900, 1050, 1200} [600] {-1800, -1400, -1000, -800, -600, -400, -300, -200, -150, -100, -50, 50, 100, 150, 200, 300, 400, 600, 800, 1000, 1400, 1800} [1000] {-2400, -1800, -1200, -900, -600, -300, -150, -50, 50, 150, 300, 600, 900, 1200, 1800, 2400}

T9(N3)	[50, 100, 150, 200, 250, 300, 400, 500, 600, 700, 900, 1000, 1200, 1400, 1600, 2000, 2500] {0} [100] {-320, -280, -240, -210, -180, -150, -120, -90, -60, -30, 30, 60, 90, 120, 150, 180, 210, 240, 280, 320} [200] {-600, -500, -400, -350, -300, -250, -200, -150, -100, -50, 50, 100, 150, 200, 250, 300, 350, 400, 500, 600} [300] {-1000, -800, -600, -500, -400, -350, -300, -250, -200, -150, -100, -50, 50, 100, 150, 200, 250, 300, 350, 400, 500, 600, 800, 1000} [400] {-1400, -1200, -1050, -900, -750, -600, -450, -300, -250, -200, -150, -100, -50, 50, 100, 150, 200, 250, 300, 450, 600, 750, 900, 1050, 1200, 1400}
dsGGACU^{A6}, 65°C, Bruker 600 MHz	
A6(C8)	[150, 200, 250, 300, 400, 500, 600, 700, 900, 1000, 1200, 1400, 1600, 2000, 2500] {0} [150] {-400, -340, -280, -240, -200, -160, -120, -80, -40, 40, 80, 120, 160, 200, 240, 280, 340, 400} [200] {-600, -500, -400, -350, -300, -250, -200, -150, -100, -50, 50, 100, 150, 200, 250, 300, 350, 400, 500, 600} [400] {-1200, -1050, -900, -750, -600, -450, -300, -250, -200, -150, -100, -50, 50, 100, 150, 200, 250, 300, 450, 600, 750, 900, 1050, 1200} [1000] {-2400, -1800, -1200, -900, -600, -300, -150, -50, 50, 150, 300, 600, 900, 1200, 1800, 2400}
dsGGACU^{m6A6}, 65°C, Bruker 600 MHz	
A6(C8)	[150, 200, 250, 300, 400, 500, 600, 700, 900, 1000, 1200, 1400, 1600, 2000, 2500] {0} [150] {-280, -240, -200, -160, -120, -80, -40, 40, 80, 120, 160, 200, 240, 280, 340, 400} [200] {-600, -500, -400, -350, -300, -250, -200, -150, -100, -50, 50, 100, 150, 200, 250, 300, 350, 400, 500, 600} [400] {-1200, -1050, -900, -750, -600, -450, -300, -250, -200, -150, -100, -50, 50, 100, 150, 200, 250, 300, 450, 600, 750, 900, 1050, 1200} [1000] {-2400, -1800, -1200, -900, -600, -300, -150, -50, 50, 150, 300, 600, 900, 1200, 1800, 2400}

Supplementary Table 6. Spin-lock power and offsets used in the CEST measurements.

Nuclei	[spin-lock power] {offset frequencies}
	$[\omega_1 2\pi^{-1}(s^{-1})]$ $\{\Omega 2\pi^{-1}(s^{-1})\}$
A_6-DNA, 45°C, Bruker 700 MHz	
C15(C1′)	[20] {-1000.0, -922.2, -844.4, -766.7, -688.9, -611.1, -533.3, -455.6, -377.8, -300.0, -300.0, -289.9, -279.7, -269.6, -259.5, -249.4, -239.2, -229.1, -219.0, -208.9, -198.7, -188.6, -178.5, -168.4, -158.2, -148.1, -138.0, -127.8, -117.7, -107.6, -97.5, -87.3, -77.2, -67.1, -57.0, -46.8, -36.7, -26.6, -16.5, -6.3, 3.8, 13.9, 24.1, 34.2, 44.3, 54.4, 64.6, 74.7, 84.8, 94.9, 105.1, 115.2, 125.3, 135.4, 145.6, 155.7, 165.8, 175.9, 186.1, 196.2, 206.3, 216.5, 226.6, 236.7, 246.8, 257.0, 267.1, 277.2, 287.3, 297.5, 307.6, 317.7, 327.8, 338.0, 348.1, 358.2, 368.4, 378.5, 388.6, 398.7, 408.9, 419.0, 429.1, 439.2, 449.4, 459.5, 469.6, 479.7, 489.9, 500.0, 500.0, 555.6, 611.1, 666.7, 722.2, 777.8, 833.3, 888.9, 944.4, 1000.0} [40] {-1000.0, -922.2, -844.4, -766.7, -688.9, -611.1, -533.3, -455.6, -377.8, -300.0, -300.0, -289.9, -279.7, -269.6, -259.5, -249.4, -239.2, -229.1, -219.0, -208.9, -198.7, -188.6, -178.5, -168.4, -158.2, -148.1, -138.0, -127.8, -117.7, -107.6, -97.5, -87.3, -77.2, -67.1, -57.0, -46.8, -36.7, -26.6, -16.5, -6.3, 3.8, 13.9, 24.1, 34.2, 44.3, 54.4, 64.6, 74.7, 84.8, 94.9, 105.1, 115.2, 125.3, 135.4, 145.6, 155.7, 165.8, 175.9, 186.1, 196.2, 206.3, 216.5, 226.6, 236.7, 246.8, 257.0, 267.1, 277.2, 287.3, 297.5, 307.6, 317.7, 327.8, 338.0, 348.1, 358.2, 368.4, 378.5, 388.6, 398.7, 408.9, 419.0, 429.1, 439.2, 449.4, 459.5, 469.6, 479.7, 489.9, 500.0, 500.0, 555.6, 611.1, 666.7, 722.2, 777.8, 833.3, 888.9, 944.4, 1000.0}
G11(C8)	[20] {-1000.0, -922.2, -844.4, -766.7, -688.9, -611.1, -533.3, -455.6, -377.8, -300.0, -300.0, -289.9, -279.7, -269.6, -259.5, -249.4, -239.2, -229.1, -219.0, -208.9, -198.7, -188.6, -178.5, -168.4, -158.2, -148.1, -138.0, -127.8, -117.7, -107.6, -97.5, -87.3, -77.2, -67.1, -57.0, -46.8, -36.7, -26.6, -16.5, -6.3, 3.8, 13.9, 24.1, 34.2, 44.3, 54.4, 64.6, 74.7, 84.8, 94.9, 105.1, 115.2, 125.3, 135.4, 145.6, 155.7, 165.8, 175.9, 186.1, 196.2, 206.3, 216.5, 226.6, 236.7, 246.8, 257.0, 267.1, 277.2, 287.3, 297.5, 307.6, 317.7, 327.8, 338.0, 348.1, 358.2, 368.4, 378.5, 388.6, 398.7, 408.9, 419.0, 429.1, 439.2, 449.4, 459.5, 469.6, 479.7, 489.9, 500.0, 500.0, 555.6, 611.1, 666.7, 722.2, 777.8, 833.3, 888.9, 944.4, 1000.0} [40] {-1000.0, -922.2, -844.4, -766.7, -688.9, -611.1, -533.3, -455.6, -377.8, -300.0, -300.0, -289.9, -279.7, -269.6, -259.5, -249.4, -239.2, -229.1, -219.0, -208.9, -198.7, -188.6, -178.5, -168.4, -158.2, -148.1, -138.0, -127.8, -117.7, -107.6, -97.5, -87.3, -77.2, -67.1, -57.0, -46.8, -36.7, -26.6, -16.5, -6.3, 3.8, 13.9, 24.1, 34.2, 44.3, 54.4, 64.6, 74.7, 84.8, 94.9, 105.1, 115.2, 125.3, 135.4, 145.6, 155.7, 165.8, 175.9, 186.1, 196.2, 206.3, 216.5, 226.6, 236.7, 246.8, 257.0, 267.1, 277.2, 287.3, 297.5, 307.6, 317.7, 327.8, 338.0, 348.1, 358.2, 368.4, 378.5, 388.6, 398.7, 408.9, 419.0, 429.1, 439.2, 449.4, 459.5, 469.6, 479.7, 489.9, 500.0, 500.0, 555.6, 611.1, 666.7, 722.2, 777.8, 833.3, 888.9, 944.4, 1000.0}
G13(C8)	[20] {-1000.0, -922.2, -844.4, -766.7, -688.9, -611.1, -533.3, -455.6, -377.8, -300.0, -300.0, -289.9, -279.7, -269.6, -259.5, -249.4, -239.2, -229.1, -219.0, -208.9, -198.7, -188.6, -178.5, -168.4, -158.2, -148.1, -138.0, -127.8, -117.7, -107.6, -97.5, -87.3, -77.2, -67.1, -57.0, -46.8, -36.7, -26.6, -16.5, -6.3, 3.8, 13.9, 24.1, 34.2, 44.3, 54.4, 64.6, 74.7, 84.8, 94.9, 105.1, 115.2, 125.3, 135.4, 145.6, 155.7, 165.8, 175.9, 186.1, 196.2, 206.3, 216.5, 226.6, 236.7, 246.8, 257.0, 267.1, 277.2, 287.3, 297.5, 307.6, 317.7, 327.8,

	338.0, 348.1, 358.2, 368.4, 378.5, 388.6, 398.7, 408.9, 419.0, 429.1, 439.2, 449.4, 459.5, 469.6, 479.7, 489.9, 500.0, 500.0, 555.6, 611.1, 666.7, 722.2, 777.8, 833.3, 888.9, 944.4, 1000.0} [40] {-1000.0, -922.2, -844.4, -766.7, -688.9, -611.1, -533.3, -455.6, -377.8, -300.0, -300.0, -289.9, -279.7, -269.6, -259.5, -249.4, -239.2, -229.1, -219.0, -208.9, -198.7, -188.6, -178.5, -168.4, -158.2, -148.1, -138.0, -127.8, -117.7, -107.6, -97.5, -87.3, -77.2, -67.1, -57.0, -46.8, -36.7, -26.6, -16.5, -6.3, 3.8, 13.9, 24.1, 34.2, 44.3, 54.4, 64.6, 74.7, 84.8, 94.9, 105.1, 115.2, 125.3, 135.4, 145.6, 155.7, 165.8, 175.9, 186.1, 196.2, 206.3, 216.5, 226.6, 236.7, 246.8, 257.0, 267.1, 277.2, 287.3, 297.5, 307.6, 317.7, 327.8, 338.0, 348.1, 358.2, 368.4, 378.5, 388.6, 398.7, 408.9, 419.0, 429.1, 439.2, 449.4, 459.5, 469.6, 479.7, 489.9, 500.0, 500.0, 555.6, 611.1, 666.7, 722.2, 777.8, 833.3, 888.9, 944.4, 1000.0}
G2(C8)	[20] {-1000.0, -922.2, -844.4, -766.7, -688.9, -611.1, -533.3, -455.6, -377.8, -300.0, -300.0, -289.9, -279.7, -269.6, -259.5, -249.4, -239.2, -229.1, -219.0, -208.9, -198.7, -188.6, -178.5, -168.4, -158.2, -148.1, -138.0, -127.8, -117.7, -107.6, -97.5, -87.3, -77.2, -67.1, -57.0, -46.8, -36.7, -26.6, -16.5, -6.3, 3.8, 13.9, 24.1, 34.2, 44.3, 54.4, 64.6, 74.7, 84.8, 94.9, 105.1, 115.2, 125.3, 135.4, 145.6, 155.7, 165.8, 175.9, 186.1, 196.2, 206.3, 216.5, 226.6, 236.7, 246.8, 257.0, 267.1, 277.2, 287.3, 297.5, 307.6, 317.7, 327.8, 338.0, 348.1, 358.2, 368.4, 378.5, 388.6, 398.7, 408.9, 419.0, 429.1, 439.2, 449.4, 459.5, 469.6, 479.7, 489.9, 500.0, 500.0, 555.6, 611.1, 666.7, 722.2, 777.8, 833.3, 888.9, 944.4, 1000.0} [40] {-1000.0, -922.2, -844.4, -766.7, -688.9, -611.1, -533.3, -455.6, -377.8, -300.0, -300.0, -289.9, -279.7, -269.6, -259.5, -249.4, -239.2, -229.1, -219.0, -208.9, -198.7, -188.6, -178.5, -168.4, -158.2, -148.1, -138.0, -127.8, -117.7, -107.6, -97.5, -87.3, -77.2, -67.1, -57.0, -46.8, -36.7, -26.6, -16.5, -6.3, 3.8, 13.9, 24.1, 34.2, 44.3, 54.4, 64.6, 74.7, 84.8, 94.9, 105.1, 115.2, 125.3, 135.4, 145.6, 155.7, 165.8, 175.9, 186.1, 196.2, 206.3, 216.5, 226.6, 236.7, 246.8, 257.0, 267.1, 277.2, 287.3, 297.5, 307.6, 317.7, 327.8, 338.0, 348.1, 358.2, 368.4, 378.5, 388.6, 398.7, 408.9, 419.0, 429.1, 439.2, 449.4, 459.5, 469.6, 479.7, 489.9, 500.0, 500.0, 555.6, 611.1, 666.7, 722.2, 777.8, 833.3, 888.9, 944.4, 1000.0}
T4(N3)	[10] {-600.0, -577.8, -555.6, -533.3, -511.1, -488.9, -466.7, -444.4, -422.2, -400.0, -400.0, -392.4, -384.8, -377.2, -369.6, -362.0, -354.4, -346.8, -339.2, -331.6, -324.1, -316.5, -308.9, -301.3, -293.7, -286.1, -278.5, -270.9, -263.3, -255.7, -248.1, -240.5, -232.9, -225.3, -217.7, -210.1, -202.5, -194.9, -187.3, -179.7, -172.2, -164.6, -157.0, -149.4, -141.8, -134.2, -126.6, -119.0, -111.4, -103.8, -96.2, -88.6, -81.0, -73.4, -65.8, -58.2, -50.6, -43.0, -35.4, -27.8, -20.3, -12.7, -5.1, 2.5, 10.1, 17.7, 25.3, 32.9, 40.5, 48.1, 55.7, 63.3, 70.9, 78.5, 86.1, 93.7, 101.3, 108.9, 116.5, 124.1, 131.6, 139.2, 146.8, 154.4, 162.0, 169.6, 177.2, 184.8, 192.4, 200.0, 200.0, 244.4, 288.9, 333.3, 377.8, 422.2, 466.7, 511.1, 555.6, 600.0} [20] {-600.0, -577.8, -555.6, -533.3, -511.1, -488.9, -466.7, -444.4, -422.2, -400.0, -400.0, -392.4, -384.8, -377.2, -369.6, -362.0, -354.4, -346.8, -339.2, -331.6, -324.1, -316.5, -308.9, -301.3, -293.7, -286.1, -278.5, -270.9, -263.3, -255.7, -248.1, -240.5, -232.9, -225.3, -217.7, -210.1, -202.5, -194.9, -187.3, -179.7, -172.2, -164.6, -157.0, -149.4, -141.8, -134.2, -126.6, -119.0, -111.4, -103.8, -96.2, -88.6, -81.0, -73.4, -65.8, -58.2, -50.6, -43.0, -35.4, -27.8, -20.3, -12.7, -5.1, 2.5, 10.1, 17.7, 25.3, 32.9, 40.5, 48.1, 55.7, 63.3, 70.9, 78.5, 86.1, 93.7, 101.3, 108.9, 116.5, 124.1, 131.6, 139.2, 146.8, 154.4, 162.0, 169.6, 177.2, 184.8, 192.4, 200.0, 200.0, 244.4, 288.9, 333.3, 377.8, 422.2, 466.7, 511.1, 555.6, 600.0}
T6(N3)	[20] {-600.0, -577.8, -555.6, -533.3, -511.1, -488.9, -466.7, -444.4, -422.2, -400.0, -400.0, -392.4, -384.8, -377.2, -369.6, -362.0, -354.4, -346.8, -339.2, -331.6, -324.1, -316.5, -308.9, -301.3, -293.7, -286.1, -278.5, -270.9, -263.3, -255.7, -248.1, -240.5, -232.9, -225.3, -217.7, -210.1, -202.5, -194.9, -187.3, -179.7, -172.2, -164.6, -157.0, -149.4, -141.8, -134.2, -126.6, -119.0, -111.4, -103.8, -96.2, -88.6, -81.0,

	-73.4, -65.8, -58.2, -50.6, -43.0, -35.4, -27.8, -20.3, -12.7, -5.1, 2.5, 10.1, 17.7, 25.3, 32.9, 40.5, 48.1, 55.7, 63.3, 70.9, 78.5, 86.1, 93.7, 101.3, 108.9, 116.5, 124.1, 131.6, 139.2, 146.8, 154.4, 162.0, 169.6, 177.2, 184.8, 192.4, 200.0, 200.0, 244.4, 288.9, 333.3, 377.8, 422.2, 466.7, 511.1, 555.6, 600.0}
T78(N3)	[10] {-600.0, -577.8, -555.6, -533.3, -511.1, -488.9, -466.7, -444.4, -422.2, -400.0, -400.0, -392.4, -384.8, -377.2, -369.6, -362.0, -354.4, -346.8, -339.2, -331.6, -324.1, -316.5, -308.9, -301.3, -293.7, -286.1, -278.5, -270.9, -263.3, -255.7, -248.1, -240.5, -232.9, -225.3, -217.7, -210.1, -202.5, -194.9, -187.3, -179.7, -172.2, -164.6, -157.0, -149.4, -141.8, -134.2, -126.6, -119.0, -111.4, -103.8, -96.2, -88.6, -81.0, -73.4, -65.8, -58.2, -50.6, -43.0, -35.4, -27.8, -20.3, -12.7, -5.1, 2.5, 10.1, 17.7, 25.3, 32.9, 40.5, 48.1, 55.7, 63.3, 70.9, 78.5, 86.1, 93.7, 101.3, 108.9, 116.5, 124.1, 131.6, 139.2, 146.8, 154.4, 162.0, 169.6, 177.2, 184.8, 192.4, 200.0, 200.0, 244.4, 288.9, 333.3, 377.8, 422.2, 466.7, 511.1, 555.6, 600.0} [20] {-600.0, -577.8, -555.6, -533.3, -511.1, -488.9, -466.7, -444.4, -422.2, -400.0, -400.0, -392.4, -384.8, -377.2, -369.6, -362.0, -354.4, -346.8, -339.2, -331.6, -324.1, -316.5, -308.9, -301.3, -293.7, -286.1, -278.5, -270.9, -263.3, -255.7, -248.1, -240.5, -232.9, -225.3, -217.7, -210.1, -202.5, -194.9, -187.3, -179.7, -172.2, -164.6, -157.0, -149.4, -141.8, -134.2, -126.6, -119.0, -111.4, -103.8, -96.2, -88.6, -81.0, -73.4, -65.8, -58.2, -50.6, -43.0, -35.4, -27.8, -20.3, -12.7, -5.1, 2.5, 10.1, 17.7, 25.3, 32.9, 40.5, 48.1, 55.7, 63.3, 70.9, 78.5, 86.1, 93.7, 101.3, 108.9, 116.5, 124.1, 131.6, 139.2, 146.8, 154.4, 162.0, 169.6, 177.2, 184.8, 192.4, 200.0, 200.0, 244.4, 288.9, 333.3, 377.8, 422.2, 466.7, 511.1, 555.6, 600.0}
T9(C1′)	[20] {-1000.0, -922.2, -844.4, -766.7, -688.9, -611.1, -533.3, -455.6, -377.8, -300.0, -300.0, -289.9, -279.7, -269.6, -259.5, -249.4, -239.2, -229.1, -219.0, -208.9, -198.7, -188.6, -178.5, -168.4, -158.2, -148.1, -138.0, -127.8, -117.7, -107.6, -97.5, -87.3, -77.2, -67.1, -57.0, -46.8, -36.7, -26.6, -16.5, -6.3, 3.8, 13.9, 24.1, 34.2, 44.3, 54.4, 64.6, 74.7, 84.8, 94.9, 105.1, 115.2, 125.3, 135.4, 145.6, 155.7, 165.8, 175.9, 186.1, 196.2, 206.3, 216.5, 226.6, 236.7, 246.8, 257.0, 267.1, 277.2, 287.3, 297.5, 307.6, 317.7, 327.8, 338.0, 348.1, 358.2, 368.4, 378.5, 388.6, 398.7, 408.9, 419.0, 429.1, 439.2, 449.4, 459.5, 469.6, 479.7, 489.9, 500.0, 500.0, 555.6, 611.1, 666.7, 722.2, 777.8, 833.3, 888.9, 944.4, 1000.0} [40] {-1000.0, -922.2, -844.4, -766.7, -688.9, -611.1, -533.3, -455.6, -377.8, -300.0, -300.0, -289.9, -279.7, -269.6, -259.5, -249.4, -239.2, -229.1, -219.0, -208.9, -198.7, -188.6, -178.5, -168.4, -158.2, -148.1, -138.0, -127.8, -117.7, -107.6, -97.5, -87.3, -77.2, -67.1, -57.0, -46.8, -36.7, -26.6, -16.5, -6.3, 3.8, 13.9, 24.1, 34.2, 44.3, 54.4, 64.6, 74.7, 84.8, 94.9, 105.1, 115.2, 125.3, 135.4, 145.6, 155.7, 165.8, 175.9, 186.1, 196.2, 206.3, 216.5, 226.6, 236.7, 246.8, 257.0, 267.1, 277.2, 287.3, 297.5, 307.6, 317.7, 327.8, 338.0, 348.1, 358.2, 368.4, 378.5, 388.6, 398.7, 408.9, 419.0, 429.1, 439.2, 449.4, 459.5, 469.6, 479.7, 489.9, 500.0, 500.0, 555.6, 611.1, 666.7, 722.2, 777.8, 833.3, 888.9, 944.4, 1000.0}
A_6-DNA, 50°C, Bruker 600 MHz	
G11(C8)	[10] {-1000.0, -922.2, -844.4, -766.7, -688.9, -611.1, -533.3, -455.6, -377.8, -300.0, -300.0, -290.7, -281.4, -272.1, -262.8, -253.4, -244.1, -234.8, -225.5, -216.2, -206.9, -197.6, -188.3, -179.0, -169.7, -160.3, -151.0, -141.7, -132.4, -123.1, -113.8, -104.5, -95.2, -85.9, -76.6, -67.2, -57.9, -48.6, -39.3, -30.0, 30.0, 39.6, 49.2, 58.8, 68.4, 78.0, 87.6, 97.1, 106.7, 116.3, 125.9, 135.5, 145.1, 154.7, 164.3, 173.9, 183.5, 193.1, 202.7, 212.2, 221.8, 231.4, 241.0, 250.6, 260.2, 269.8, 279.4, 289.0, 298.6, 308.2, 317.8, 327.3, 336.9, 346.5, 356.1, 365.7, 375.3, 384.9, 394.5, 404.1, 413.7, 423.3, 432.9, 442.4, 452.0, 461.6, 471.2, 480.8, 490.4, 500.0, 500.0, 555.6, 611.1, 666.7, 722.2, 777.8, 833.3, 888.9, 944.4, 1000.0} [25] {-942.9, -878.6, -814.3, -750.0, -685.7, -621.4, -557.1, -492.9, -428.6, -364.3, -300.0, -300.0, -283.7, -267.3, -251.0, -234.7, -218.4, -202.0, -185.7, -169.4, -153.1, -136.7, -120.4, -104.1, -87.8, -71.4, -55.1,

	-38.8, -22.4, -6.1, 10.2, 26.5, 42.9, 59.2, 75.5, 91.8, 108.2, 124.5, 140.8, 157.1, 173.5, 189.8, 206.1, 222.4, 238.8, 255.1, 271.4, 287.8, 304.1, 320.4, 336.7, 353.1, 369.4, 385.7, 402.0, 418.4, 434.7, 451.0, 467.3, 483.7, 500.0, 500.0, 550.0, 600.0, 650.0, 700.0, 750.0, 800.0, 850.0, 900.0, 950.0, 1000.0}
A_2-DNA, 50°C, Bruker 600 MHz	
G11(C8)	[10] {-1000.0, -963.2, -926.3, -889.5, -852.6, -815.8, -778.9, -742.1, -705.3, -668.4, -631.6, -594.7, -557.9, -521.1, -484.2, -447.4, -410.5, -373.7, -336.8, -300.0, -300.0, -291.9, -283.8, -275.8, -267.7, -259.6, -251.5, -243.4, -235.4, -227.3, -219.2, -211.1, -203.0, -194.9, -186.9, -178.8, -170.7, -162.6, -154.5, -146.5, -138.4, -130.3, -122.2, -114.1, -106.1, -98.0, -89.9, -81.8, -73.7, -65.7, -57.6, -49.5, -41.4, -33.3, -25.3, -17.2, -9.1, -1.0, 7.1, 15.2, 23.2, 31.3, 39.4, 47.5, 55.6, 63.6, 71.7, 79.8, 87.9, 96.0, 104.0, 112.1, 120.2, 128.3, 136.4, 144.4, 152.5, 160.6, 168.7, 176.8, 184.8, 192.9, 201.0, 209.1, 217.2, 225.3, 233.3, 241.4, 249.5, 257.6, 265.7, 273.7, 281.8, 289.9, 298.0, 306.1, 314.1, 322.2, 330.3, 338.4, 346.5, 354.5, 362.6, 370.7, 378.8, 386.9, 394.9, 403.0, 411.1, 419.2, 427.3, 435.4, 443.4, 451.5, 459.6, 467.7, 475.8, 483.8, 491.9, 500.0, 500.0, 526.3, 552.6, 578.9, 605.3, 631.6, 657.9, 684.2, 710.5, 736.8, 763.2, 789.5, 815.8, 842.1, 868.4, 894.7, 921.1, 947.4, 973.7, 1000.0} [25] {-1000.0, -963.2, -926.3, -889.5, -852.6, -815.8, -778.9, -742.1, -705.3, -668.4, -631.6, -594.7, -557.9, -521.1, -484.2, -447.4, -410.5, -373.7, -336.8, -300.0, -300.0, -291.9, -283.8, -275.8, -267.7, -259.6, -251.5, -243.4, -235.4, -227.3, -219.2, -211.1, -203.0, -194.9, -186.9, -178.8, -170.7, -162.6, -154.5, -146.5, -138.4, -130.3, -122.2, -114.1, -106.1, -98.0, -89.9, -81.8, -73.7, -65.7, -57.6, -49.5, -41.4, -33.3, -25.3, -17.2, -9.1, -1.0, 7.1, 15.2, 23.2, 31.3, 39.4, 47.5, 55.6, 63.6, 71.7, 79.8, 87.9, 96.0, 104.0, 112.1, 120.2, 128.3, 136.4, 144.4, 152.5, 160.6, 168.7, 176.8, 184.8, 192.9, 201.0, 209.1, 217.2, 225.3, 233.3, 241.4, 249.5, 257.6, 265.7, 273.7, 281.8, 289.9, 298.0, 306.1, 314.1, 322.2, 330.3, 338.4, 346.5, 354.5, 362.6, 370.7, 378.8, 386.9, 394.9, 403.0, 411.1, 419.2, 427.3, 435.4, 443.4, 451.5, 459.6, 467.7, 475.8, 483.8, 491.9, 500.0, 500.0, 526.3, 552.6, 578.9, 605.3, 631.6, 657.9, 684.2, 710.5, 736.8, 763.2, 789.5, 815.8, 842.1, 868.4, 894.7, 921.1, 947.4, 973.7, 1000.0}
dsGGACU^{A6}, 65°C, no Mg^{2+}, Bruker 600 MHz	
A6(C2)	[10] {-1000.0, -944.4, -888.9, -833.3, -777.8, -722.2, -666.7, -611.1, -555.6, -500.0, -500.0, -487.3, -474.7, -462.0, -449.4, -436.7, -424.1, -411.4, -398.7, -386.1, -373.4, -360.8, -348.1, -335.4, -322.8, -310.1, -297.5, -284.8, -272.2, -259.5, -246.8, -234.2, -221.5, -208.9, -196.2, -183.5, -170.9, -158.2, -145.6, -132.9, -120.3, -107.6, -94.9, -82.3, -69.6, -57.0, -44.3, -31.6, -19.0, -6.3, 6.3, 19.0, 31.6, 44.3, 57.0, 69.6, 82.3, 94.9, 107.6, 120.3, 132.9, 145.6, 158.2, 170.9, 183.5, 196.2, 208.9, 221.5, 234.2, 246.8, 259.5, 272.2, 284.8, 297.5, 310.1, 322.8, 335.4, 348.1, 360.8, 373.4, 386.1, 398.7, 411.4, 424.1, 436.7, 449.4, 462.0, 474.7, 487.3, 500.0, 500.0, 555.6, 611.1, 666.7, 722.2, 777.8, 833.3, 888.9, 944.4, 1000.0} [20] {-1000.0, -944.4, -888.9, -833.3, -777.8, -722.2, -666.7, -611.1, -555.6, -500.0, -500.0, -487.3, -474.7, -462.0, -449.4, -436.7, -424.1, -411.4, -398.7, -386.1, -373.4, -360.8, -348.1, -335.4, -322.8, -310.1, -297.5, -284.8, -272.2, -259.5, -246.8, -234.2, -221.5, -208.9, -196.2, -183.5, -170.9, -158.2, -145.6, -132.9, -120.3, -107.6, -94.9, -82.3, -69.6, -57.0, -44.3, -31.6, -19.0, -6.3, 6.3, 19.0, 31.6, 44.3, 57.0, 69.6, 82.3, 94.9, 107.6, 120.3, 132.9, 145.6, 158.2, 170.9, 183.5, 196.2, 208.9, 221.5, 234.2, 246.8, 259.5, 272.2, 284.8, 297.5, 310.1, 322.8, 335.4, 348.1, 360.8, 373.4, 386.1, 398.7, 411.4, 424.1, 436.7, 449.4, 462.0, 474.7, 487.3, 500.0, 500.0, 555.6, 611.1, 666.7, 722.2, 777.8, 833.3, 888.9, 944.4, 1000.0}

A6(C8)	[20] {-1000.0, -944.4, -888.9, -833.3, -777.8, -722.2, -666.7, -611.1, -555.6, -500.0, -500.0, -487.3, -474.7, -462.0, -449.4, -436.7, -424.1, -411.4, -398.7, -386.1, -373.4, -360.8, -348.1, -335.4, -322.8, -310.1, -297.5, -284.8, -272.2, -259.5, -246.8, -234.2, -221.5, -208.9, -196.2, -183.5, -170.9, -158.2, -145.6, -132.9, -120.3, -107.6, -94.9, -82.3, -69.6, -57.0, -44.3, -31.6, -19.0, -6.3, 6.3, 19.0, 31.6, 44.3, 57.0, 69.6, 82.3, 94.9, 107.6, 120.3, 132.9, 145.6, 158.2, 170.9, 183.5, 196.2, 208.9, 221.5, 234.2, 246.8, 259.5, 272.2, 284.8, 297.5, 310.1, 322.8, 335.4, 348.1, 360.8, 373.4, 386.1, 398.7, 411.4, 424.1, 436.7, 449.4, 462.0, 474.7, 487.3, 500.0, 500.0, 555.6, 611.1, 666.7, 722.2, 777.8, 833.3, 888.9, 944.4, 1000.0} [40] {-1000.0, -944.4, -888.9, -833.3, -777.8, -722.2, -666.7, -611.1, -555.6, -500.0, -500.0, -487.3, -474.7, -462.0, -449.4, -436.7, -424.1, -411.4, -398.7, -386.1, -373.4, -360.8, -348.1, -335.4, -322.8, -310.1, -297.5, -284.8, -272.2, -259.5, -246.8, -234.2, -221.5, -208.9, -196.2, -183.5, -170.9, -158.2, -145.6, -132.9, -120.3, -107.6, -94.9, -82.3, -69.6, -57.0, -44.3, -31.6, -19.0, -6.3, 6.3, 19.0, 31.6, 44.3, 57.0, 69.6, 82.3, 94.9, 107.6, 120.3, 132.9, 145.6, 158.2, 170.9, 183.5, 196.2, 208.9, 221.5, 234.2, 246.8, 259.5, 272.2, 284.8, 297.5, 310.1, 322.8, 335.4, 348.1, 360.8, 373.4, 386.1, 398.7, 411.4, 424.1, 436.7, 449.4, 462.0, 474.7, 487.3, 500.0, 500.0, 555.6, 611.1, 666.7, 722.2, 777.8, 833.3, 888.9, 944.4, 1000.0}
dsGGACU^{m6A6}, 65°C, no Mg^{2+}, Bruker 600 MHz	
A6(C2)	[10] {-1000.0, -922.2, -844.4, -766.7, -688.9, -611.1, -533.3, -455.6, -377.8, -300.0, -300.0, -286.4, -272.9, -259.3, -245.8, -232.2, -218.6, -205.1, -191.5, -178.0, -164.4, -150.8, -137.3, -123.7, -110.2, -96.6, -83.1, -69.5, -55.9, -42.4, -28.8, -15.3, -1.7, 11.9, 25.4, 39.0, 52.5, 66.1, 79.7, 93.2, 106.8, 120.3, 133.9, 147.5, 161.0, 174.6, 188.1, 201.7, 215.3, 228.8, 242.4, 255.9, 269.5, 283.1, 296.6, 310.2, 323.7, 337.3, 350.8, 364.4, 378.0, 391.5, 405.1, 418.6, 432.2, 445.8, 459.3, 472.9, 486.4, 500.0, 500.0, 555.6, 611.1, 666.7, 722.2, 777.8, 833.3, 888.9, 944.4, 1000.0} [20] {-1000.0, -922.2, -844.4, -766.7, -688.9, -611.1, -533.3, -455.6, -377.8, -300.0, -300.0, -286.4, -272.9, -259.3, -245.8, -232.2, -218.6, -205.1, -191.5, -178.0, -164.4, -150.8, -137.3, -123.7, -110.2, -96.6, -83.1, -69.5, -55.9, -42.4, -28.8, -15.3, -1.7, 11.9, 25.4, 39.0, 52.5, 66.1, 79.7, 93.2, 106.8, 120.3, 133.9, 147.5, 161.0, 174.6, 188.1, 201.7, 215.3, 228.8, 242.4, 255.9, 269.5, 283.1, 296.6, 310.2, 323.7, 337.3, 350.8, 364.4, 378.0, 391.5, 405.1, 418.6, 432.2, 445.8, 459.3, 472.9, 486.4, 500.0, 500.0, 555.6, 611.1, 666.7, 722.2, 777.8, 833.3, 888.9, 944.4, 1000.0}
A6(C8)	[20] {-1000.0, -922.2, -844.4, -766.7, -688.9, -611.1, -533.3, -455.6, -377.8, -300.0, -300.0, -286.4, -272.9, -259.3, -245.8, -232.2, -218.6, -205.1, -191.5, -178.0, -164.4, -150.8, -137.3, -123.7, -110.2, -96.6, -83.1, -69.5, -55.9, -42.4, -28.8, -15.3, -1.7, 11.9, 25.4, 39.0, 52.5, 66.1, 79.7, 93.2, 106.8, 120.3, 133.9, 147.5, 161.0, 174.6, 188.1, 201.7, 215.3, 228.8, 242.4, 255.9, 269.5, 283.1, 296.6, 310.2, 323.7, 337.3, 350.8, 364.4, 378.0, 391.5, 405.1, 418.6, 432.2, 445.8, 459.3, 472.9, 486.4, 500.0, 500.0, 555.6, 611.1, 666.7, 722.2, 777.8, 833.3, 888.9, 944.4, 1000.0} [40] {-1000.0, -922.2, -844.4, -766.7, -688.9, -611.1, -533.3, -455.6, -377.8, -300.0, -300.0, -279.5, -259.0, -238.5, -217.9, -197.4, -176.9, -156.4, -135.9, -115.4, -94.9, -74.4, -53.8, -33.3, -12.8, 7.7, 28.2, 48.7, 69.2, 89.7, 110.3, 130.8, 151.3, 171.8, 192.3, 212.8, 233.3, 253.8, 274.4, 294.9, 315.4, 335.9, 356.4, 376.9, 397.4, 417.9, 438.5, 459.0, 479.5, 500.0, 500.0, 555.6, 611.1, 666.7, 722.2, 777.8, 833.3, 888.9, 944.4, 1000.0, -1000.0, -922.2, -844.4, -766.7, -688.9, -611.1, -533.3, -455.6, -377.8, -300.0, -300.0, -279.5, -259.0, -238.5, -217.9, -197.4, -176.9, -156.4, -135.9, -115.4, -94.9, -74.4, -53.8, -33.3, -12.8, 7.7, 28.2, 48.7, 69.2, 89.7, 110.3, 130.8, 151.3, 171.8, 192.3, 212.8, 233.3, 253.8, 274.4, 294.9, 315.4, 335.9, 356.4, 376.9, 397.4, 417.9, 438.5, 459.0, 479.5, 500.0, 500.0, 555.6, 611.1, 666.7, 722.2, 777.8, 833.3, 888.9,

	944.4, 1000.0}
dsGGACU^{A6}, 65°C, Mg^{2+}, Bruker 600 MHz	
A6(C2)	[10] {-1000.0, -922.2, -844.4, -766.7, -688.9, -611.1, -533.3, -455.6, -377.8, -300.0, -300.0, -290.7, -281.4, -272.1, -262.8, -253.4, -244.1, -234.8, -225.5, -216.2, -206.9, -197.6, -188.3, -179.0, -169.7, -160.3, -151.0, -141.7, -132.4, -123.1, -113.8, -104.5, -95.2, -85.9, -76.6, -67.2, -57.9, -48.6, -39.3, -30.0, 30.0, 39.6, 49.2, 58.8, 68.4, 78.0, 87.6, 97.1, 106.7, 116.3, 125.9, 135.5, 145.1, 154.7, 164.3, 173.9, 183.5, 193.1, 202.7, 212.2, 221.8, 231.4, 241.0, 250.6, 260.2, 269.8, 279.4, 289.0, 298.6, 308.2, 317.8, 327.3, 336.9, 346.5, 356.1, 365.7, 375.3, 384.9, 394.5, 404.1, 413.7, 423.3, 432.9, 442.4, 452.0, 461.6, 471.2, 480.8, 490.4, 500.0, 500.0, 555.6, 611.1, 666.7, 722.2, 777.8, 833.3, 888.9, 944.4, 1000.0} [20] {-1000.0, -922.2, -844.4, -766.7, -688.9, -611.1, -533.3, -455.6, -377.8, -300.0, -300.0, -290.7, -281.4, -272.1, -262.8, -253.4, -244.1, -234.8, -225.5, -216.2, -206.9, -197.6, -188.3, -179.0, -169.7, -160.3, -151.0, -141.7, -132.4, -123.1, -113.8, -104.5, -95.2, -85.9, -76.6, -67.2, -57.9, -48.6, -39.3, -30.0, 30.0, 39.6, 49.2, 58.8, 68.4, 78.0, 87.6, 97.1, 106.7, 116.3, 125.9, 135.5, 145.1, 154.7, 164.3, 173.9, 183.5, 193.1, 202.7, 212.2, 221.8, 231.4, 241.0, 250.6, 260.2, 269.8, 279.4, 289.0, 298.6, 308.2, 317.8, 327.3, 336.9, 346.5, 356.1, 365.7, 375.3, 384.9, 394.5, 404.1, 413.7, 423.3, 432.9, 442.4, 452.0, 461.6, 471.2, 480.8, 490.4, 500.0, 500.0, 555.6, 611.1, 666.7, 722.2, 777.8, 833.3, 888.9, 944.4, 1000.0} [40] {-1000.0, -922.2, -844.4, -766.7, -688.9, -611.1, -533.3, -455.6, -377.8, -300.0, -300.0, -290.7, -281.4, -272.1, -262.8, -253.4, -244.1, -234.8, -225.5, -216.2, -206.9, -197.6, -188.3, -179.0, -169.7, -160.3, -151.0, -141.7, -132.4, -123.1, -113.8, -104.5, -95.2, -85.9, -76.6, -67.2, -57.9, -48.6, -39.3, -30.0, 30.0, 39.6, 49.2, 58.8, 68.4, 78.0, 87.6, 97.1, 106.7, 116.3, 125.9, 135.5, 145.1, 154.7, 164.3, 173.9, 183.5, 193.1, 202.7, 212.2, 221.8, 231.4, 241.0, 250.6, 260.2, 269.8, 279.4, 289.0, 298.6, 308.2, 317.8, 327.3, 336.9, 346.5, 356.1, 365.7, 375.3, 384.9, 394.5, 404.1, 413.7, 423.3, 432.9, 442.4, 452.0, 461.6, 471.2, 480.8, 490.4, 500.0, 500.0, 555.6, 611.1, 666.7, 722.2, 777.8, 833.3, 888.9, 944.4, 1000.0}
A6(C8)	[10] {-1000.0, -922.2, -844.4, -766.7, -688.9, -611.1, -533.3, -455.6, -377.8, -300.0, -300.0, -290.7, -281.4, -272.1, -262.8, -253.4, -244.1, -234.8, -225.5, -216.2, -206.9, -197.6, -188.3, -179.0, -169.7, -160.3, -151.0, -141.7, -132.4, -123.1, -113.8, -104.5, -95.2, -85.9, -76.6, -67.2, -57.9, -48.6, -39.3, -30.0, 30.0, 39.6, 49.2, 58.8, 68.4, 78.0, 87.6, 97.1, 106.7, 116.3, 125.9, 135.5, 145.1, 154.7, 164.3, 173.9, 183.5, 193.1, 202.7, 212.2, 221.8, 231.4, 241.0, 250.6, 260.2, 269.8, 279.4, 289.0, 298.6, 308.2, 317.8, 327.3, 336.9, 346.5, 356.1, 365.7, 375.3, 384.9, 394.5, 404.1, 413.7, 423.3, 432.9, 442.4, 452.0, 461.6, 471.2, 480.8, 490.4, 500.0, 500.0, 555.6, 611.1, 666.7, 722.2, 777.8, 833.3, 888.9, 944.4, 1000.0} [20] {-1000.0, -922.2, -844.4, -766.7, -688.9, -611.1, -533.3, -455.6, -377.8, -300.0, -300.0, -290.7, -281.4, -272.1, -262.8, -253.4, -244.1, -234.8, -225.5, -216.2, -206.9, -197.6, -188.3, -179.0, -169.7, -160.3, -151.0, -141.7, -132.4, -123.1, -113.8, -104.5, -95.2, -85.9, -76.6, -67.2, -57.9, -48.6, -39.3, -30.0, 30.0, 39.6, 49.2, 58.8, 68.4, 78.0, 87.6, 97.1, 106.7, 116.3, 125.9, 135.5, 145.1, 154.7, 164.3, 173.9, 183.5, 193.1, 202.7, 212.2, 221.8, 231.4, 241.0, 250.6, 260.2, 269.8, 279.4, 289.0, 298.6, 308.2, 317.8, 327.3, 336.9, 346.5, 356.1, 365.7, 375.3, 384.9, 394.5, 404.1, 413.7, 423.3, 432.9, 442.4, 452.0, 461.6, 471.2, 480.8, 490.4, 500.0, 500.0, 555.6, 611.1, 666.7, 722.2, 777.8, 833.3, 888.9, 944.4, 1000.0} [40] {-1000.0, -922.2, -844.4, -766.7, -688.9, -611.1, -533.3, -455.6, -377.8, -300.0, -300.0, -290.7, -281.4, -272.1, -262.8, -253.4, -244.1, -234.8, -225.5, -216.2, -206.9, -197.6, -188.3, -179.0, -169.7, -160.3, -151.0, -141.7, -132.4, -123.1, -113.8, -104.5, -95.2, -85.9, -76.6, -67.2, -57.9, -48.6, -39.3, -30.0, 30.0, 39.6, 49.2, 58.8, 68.4, 78.0, 87.6, 97.1, 106.7, 116.3, 125.9, 135.5, 145.1, 154.7, 164.3, 173.9, 183.5,

	193.1, 202.7, 212.2, 221.8, 231.4, 241.0, 250.6, 260.2, 269.8, 279.4, 289.0, 298.6, 308.2, 317.8, 327.3, 336.9, 346.5, 356.1, 365.7, 375.3, 384.9, 394.5, 404.1, 413.7, 423.3, 432.9, 442.4, 452.0, 461.6, 471.2, 480.8, 490.4, 500.0, 500.0, 555.6, 611.1, 666.7, 722.2, 777.8, 833.3, 888.9, 944.4, 1000.0}
dsGGACU^{m6A6}, 65°C, Mg^{2+}, Bruker 600 MHz	
A6(C2)	[10] {-1000.0, -922.2, -844.4, -766.7, -688.9, -611.1, -533.3, -455.6, -377.8, -300.0, -300.0, -290.7, -281.4, -272.1, -262.8, -253.4, -244.1, -234.8, -225.5, -216.2, -206.9, -197.6, -188.3, -179.0, -169.7, -160.3, -151.0, -141.7, -132.4, -123.1, -113.8, -104.5, -95.2, -85.9, -76.6, -67.2, -57.9, -48.6, -39.3, -30.0, 30.0, 39.6, 49.2, 58.8, 68.4, 78.0, 87.6, 97.1, 106.7, 116.3, 125.9, 135.5, 145.1, 154.7, 164.3, 173.9, 183.5, 193.1, 202.7, 212.2, 221.8, 231.4, 241.0, 250.6, 260.2, 269.8, 279.4, 289.0, 298.6, 308.2, 317.8, 327.3, 336.9, 346.5, 356.1, 365.7, 375.3, 384.9, 394.5, 404.1, 413.7, 423.3, 432.9, 442.4, 452.0, 461.6, 471.2, 480.8, 490.4, 500.0, 500.0, 555.6, 611.1, 666.7, 722.2, 777.8, 833.3, 888.9, 944.4, 1000.0} [20] {-1000.0, -922.2, -844.4, -766.7, -688.9, -611.1, -533.3, -455.6, -377.8, -300.0, -300.0, -290.7, -281.4, -272.1, -262.8, -253.4, -244.1, -234.8, -225.5, -216.2, -206.9, -197.6, -188.3, -179.0, -169.7, -160.3, -151.0, -141.7, -132.4, -123.1, -113.8, -104.5, -95.2, -85.9, -76.6, -67.2, -57.9, -48.6, -39.3, -30.0, 30.0, 39.6, 49.2, 58.8, 68.4, 78.0, 87.6, 97.1, 106.7, 116.3, 125.9, 135.5, 145.1, 154.7, 164.3, 173.9, 183.5, 193.1, 202.7, 212.2, 221.8, 231.4, 241.0, 250.6, 260.2, 269.8, 279.4, 289.0, 298.6, 308.2, 317.8, 327.3, 336.9, 346.5, 356.1, 365.7, 375.3, 384.9, 394.5, 404.1, 413.7, 423.3, 432.9, 442.4, 452.0, 461.6, 471.2, 480.8, 490.4, 500.0, 500.0, 555.6, 611.1, 666.7, 722.2, 777.8, 833.3, 888.9, 944.4, 1000.0} [40] {-1000.0, -922.2, -844.4, -766.7, -688.9, -611.1, -533.3, -455.6, -377.8, -300.0, -300.0, -290.7, -281.4, -272.1, -262.8, -253.4, -244.1, -234.8, -225.5, -216.2, -206.9, -197.6, -188.3, -179.0, -169.7, -160.3, -151.0, -141.7, -132.4, -123.1, -113.8, -104.5, -95.2, -85.9, -76.6, -67.2, -57.9, -48.6, -39.3, -30.0, 30.0, 39.6, 49.2, 58.8, 68.4, 78.0, 87.6, 97.1, 106.7, 116.3, 125.9, 135.5, 145.1, 154.7, 164.3, 173.9, 183.5, 193.1, 202.7, 212.2, 221.8, 231.4, 241.0, 250.6, 260.2, 269.8, 279.4, 289.0, 298.6, 308.2, 317.8, 327.3, 336.9, 346.5, 356.1, 365.7, 375.3, 384.9, 394.5, 404.1, 413.7, 423.3, 432.9, 442.4, 452.0, 461.6, 471.2, 480.8, 490.4, 500.0, 500.0, 555.6, 611.1, 666.7, 722.2, 777.8, 833.3, 888.9, 944.4, 1000.0}
A6(C8)	[10] {-1000.0, -922.2, -844.4, -766.7, -688.9, -611.1, -533.3, -455.6, -377.8, -300.0, -300.0, -290.7, -281.4, -272.1, -262.8, -253.4, -244.1, -234.8, -225.5, -216.2, -206.9, -197.6, -188.3, -179.0, -169.7, -160.3, -151.0, -141.7, -132.4, -123.1, -113.8, -104.5, -95.2, -85.9, -76.6, -67.2, -57.9, -48.6, -39.3, -30.0, 30.0, 39.6, 49.2, 58.8, 68.4, 78.0, 87.6, 97.1, 106.7, 116.3, 125.9, 135.5, 145.1, 154.7, 164.3, 173.9, 183.5, 193.1, 202.7, 212.2, 221.8, 231.4, 241.0, 250.6, 260.2, 269.8, 279.4, 289.0, 298.6, 308.2, 317.8, 327.3, 336.9, 346.5, 356.1, 365.7, 375.3, 384.9, 394.5, 404.1, 413.7, 423.3, 432.9, 442.4, 452.0, 461.6, 471.2, 480.8, 490.4, 500.0, 500.0, 555.6, 611.1, 666.7, 722.2, 777.8, 833.3, 888.9, 944.4, 1000.0} [20] {-1000.0, -922.2, -844.4, -766.7, -688.9, -611.1, -533.3, -455.6, -377.8, -300.0, -300.0, -290.7, -281.4, -272.1, -262.8, -253.4, -244.1, -234.8, -225.5, -216.2, -206.9, -197.6, -188.3, -179.0, -169.7, -160.3, -151.0, -141.7, -132.4, -123.1, -113.8, -104.5, -95.2, -85.9, -76.6, -67.2, -57.9, -48.6, -39.3, -30.0, 30.0, 39.6, 49.2, 58.8, 68.4, 78.0, 87.6, 97.1, 106.7, 116.3, 125.9, 135.5, 145.1, 154.7, 164.3, 173.9, 183.5, 193.1, 202.7, 212.2, 221.8, 231.4, 241.0, 250.6, 260.2, 269.8, 279.4, 289.0, 298.6, 308.2, 317.8, 327.3, 336.9, 346.5, 356.1, 365.7, 375.3, 384.9, 394.5, 404.1, 413.7, 423.3, 432.9, 442.4, 452.0, 461.6, 471.2, 480.8, 490.4, 500.0, 500.0, 555.6, 611.1, 666.7, 722.2, 777.8, 833.3, 888.9, 944.4, 1000.0} [40] {-1000.0, -922.2, -844.4, -766.7, -688.9, -611.1, -533.3, -455.6, -377.8, -300.0, -300.0, -290.7, -281.4, -272.1, -262.8, -253.4, -244.1, -234.8, -225.5, -216.2, -206.9, -197.6, -188.3, -179.0, -169.7, -160.3,

	-151.0, -141.7, -132.4, -123.1, -113.8, -104.5, -95.2, -85.9, -76.6, -67.2, -57.9, -48.6, -39.3, -30.0, 30.0, 39.6, 49.2, 58.8, 68.4, 78.0, 87.6, 97.1, 106.7, 116.3, 125.9, 135.5, 145.1, 154.7, 164.3, 173.9, 183.5, 193.1, 202.7, 212.2, 221.8, 231.4, 241.0, 250.6, 260.2, 269.8, 279.4, 289.0, 298.6, 308.2, 317.8, 327.3, 336.9, 346.5, 356.1, 365.7, 375.3, 384.9, 394.5, 404.1, 413.7, 423.3, 432.9, 442.4, 452.0, 461.6, 471.2, 480.8, 490.4, 500.0, 500.0, 555.6, 611.1, 666.7, 722.2, 777.8, 833.3, 888.9, 944.4, 1000.0}
dsHCV^{A15}, 65°C, Mg^{2+}, Bruker 600 MHz	
A15(C8)	[10] {-1000.0, -922.2, -844.4, -766.7, -688.9, -611.1, -533.3, -455.6, -377.8, -300.0, -300.0, -290.7, -281.4, -272.1, -262.8, -253.4, -244.1, -234.8, -225.5, -216.2, -206.9, -197.6, -188.3, -179.0, -169.7, -160.3, -151.0, -141.7, -132.4, -123.1, -113.8, -104.5, -95.2, -85.9, -76.6, -67.2, -57.9, -48.6, -39.3, -30.0, 30.0, 39.6, 49.2, 58.8, 68.4, 78.0, 87.6, 97.1, 106.7, 116.3, 125.9, 135.5, 145.1, 154.7, 164.3, 173.9, 183.5, 193.1, 202.7, 212.2, 221.8, 231.4, 241.0, 250.6, 260.2, 269.8, 279.4, 289.0, 298.6, 308.2, 317.8, 327.3, 336.9, 346.5, 356.1, 365.7, 375.3, 384.9, 394.5, 404.1, 413.7, 423.3, 432.9, 442.4, 452.0, 461.6, 471.2, 480.8, 490.4, 500.0, 500.0, 555.6, 611.1, 666.7, 722.2, 777.8, 833.3, 888.9, 944.4, 1000.0} [20] {-1000.0, -922.2, -844.4, -766.7, -688.9, -611.1, -533.3, -455.6, -377.8, -300.0, -300.0, -290.7, -281.4, -272.1, -262.8, -253.4, -244.1, -234.8, -225.5, -216.2, -206.9, -197.6, -188.3, -179.0, -169.7, -160.3, -151.0, -141.7, -132.4, -123.1, -113.8, -104.5, -95.2, -85.9, -76.6, -67.2, -57.9, -48.6, -39.3, -30.0, 30.0, 39.6, 49.2, 58.8, 68.4, 78.0, 87.6, 97.1, 106.7, 116.3, 125.9, 135.5, 145.1, 154.7, 164.3, 173.9, 183.5, 193.1, 202.7, 212.2, 221.8, 231.4, 241.0, 250.6, 260.2, 269.8, 279.4, 289.0, 298.6, 308.2, 317.8, 327.3, 336.9, 346.5, 356.1, 365.7, 375.3, 384.9, 394.5, 404.1, 413.7, 423.3, 432.9, 442.4, 452.0, 461.6, 471.2, 480.8, 490.4, 500.0, 500.0, 555.6, 611.1, 666.7, 722.2, 777.8, 833.3, 888.9, 944.4, 1000.0} [40] {-1000.0, -922.2, -844.4, -766.7, -688.9, -611.1, -533.3, -455.6, -377.8, -300.0, -300.0, -290.7, -281.4, -272.1, -262.8, -253.4, -244.1, -234.8, -225.5, -216.2, -206.9, -197.6, -188.3, -179.0, -169.7, -160.3, -151.0, -141.7, -132.4, -123.1, -113.8, -104.5, -95.2, -85.9, -76.6, -67.2, -57.9, -48.6, -39.3, -30.0, 30.0, 39.6, 49.2, 58.8, 68.4, 78.0, 87.6, 97.1, 106.7, 116.3, 125.9, 135.5, 145.1, 154.7, 164.3, 173.9, 183.5, 193.1, 202.7, 212.2, 221.8, 231.4, 241.0, 250.6, 260.2, 269.8, 279.4, 289.0, 298.6, 308.2, 317.8, 327.3, 336.9, 346.5, 356.1, 365.7, 375.3, 384.9, 394.5, 404.1, 413.7, 423.3, 432.9, 442.4, 452.0, 461.6, 471.2, 480.8, 490.4, 500.0, 500.0, 555.6, 611.1, 666.7, 722.2, 777.8, 833.3, 888.9, 944.4, 1000.0}
dsHCV^{m6A6,A15}, 65°C, Mg^{2+}, Bruker 600 MHz	

A15(C8)	[10] {-1000.0, -922.2, -844.4, -766.7, -688.9, -611.1, -533.3, -455.6, -377.8, -300.0, -300.0, -290.7, -281.4, -272.1, -262.8, -253.4, -244.1, -234.8, -225.5, -216.2, -206.9, -197.6, -188.3, -179.0, -169.7, -160.3, -151.0, -141.7, -132.4, -123.1, -113.8, -104.5, -95.2, -85.9, -76.6, -67.2, -57.9, -48.6, -39.3, -30.0, 30.0, 39.6, 49.2, 58.8, 68.4, 78.0, 87.6, 97.1, 106.7, 116.3, 125.9, 135.5, 145.1, 154.7, 164.3, 173.9, 183.5, 193.1, 202.7, 212.2, 221.8, 231.4, 241.0, 250.6, 260.2, 269.8, 279.4, 289.0, 298.6, 308.2, 317.8, 327.3, 336.9, 346.5, 356.1, 365.7, 375.3, 384.9, 394.5, 404.1, 413.7, 423.3, 432.9, 442.4, 452.0, 461.6, 471.2, 480.8, 490.4, 500.0, 500.0, 555.6, 611.1, 666.7, 722.2, 777.8, 833.3, 888.9, 944.4, 1000.0} [20] {-1000.0, -922.2, -844.4, -766.7, -688.9, -611.1, -533.3, -455.6, -377.8, -300.0, -300.0, -290.7, -281.4, -272.1, -262.8, -253.4, -244.1, -234.8, -225.5, -216.2, -206.9, -197.6, -188.3, -179.0, -169.7, -160.3, -151.0, -141.7, -132.4, -123.1, -113.8, -104.5, -95.2, -85.9, -76.6, -67.2, -57.9, -48.6, -39.3, -30.0, 30.0, 39.6, 49.2, 58.8, 68.4, 78.0, 87.6, 97.1, 106.7, 116.3, 125.9, 135.5, 145.1, 154.7, 164.3, 173.9, 183.5, 193.1, 202.7, 212.2, 221.8, 231.4, 241.0, 250.6, 260.2, 269.8, 279.4, 289.0, 298.6, 308.2, 317.8, 327.3, 336.9, 346.5, 356.1, 365.7, 375.3, 384.9, 394.5, 404.1, 413.7, 423.3, 432.9, 442.4, 452.0, 461.6, 471.2, 480.8, 490.4, 500.0, 500.0, 555.6, 611.1, 666.7, 722.2, 777.8, 833.3, 888.9, 944.4, 1000.0} [40] {-1000.0, -922.2, -844.4, -766.7, -688.9, -611.1, -533.3, -455.6, -377.8, -300.0, -300.0, -290.7, -281.4, -272.1, -262.8, -253.4, -244.1, -234.8, -225.5, -216.2, -206.9, -197.6, -188.3, -179.0, -169.7, -160.3, -151.0, -141.7, -132.4, -123.1, -113.8, -104.5, -95.2, -85.9, -76.6, -67.2, -57.9, -48.6, -39.3, -30.0, 30.0, 39.6, 49.2, 58.8, 68.4, 78.0, 87.6, 97.1, 106.7, 116.3, 125.9, 135.5, 145.1, 154.7, 164.3, 173.9, 183.5, 193.1, 202.7, 212.2, 221.8, 231.4, 241.0, 250.6, 260.2, 269.8, 279.4, 289.0, 298.6, 308.2, 317.8, 327.3, 336.9, 346.5, 356.1, 365.7, 375.3, 384.9, 394.5, 404.1, 413.7, 423.3, 432.9, 442.4, 452.0, 461.6, 471.2, 480.8, 490.4, 500.0, 500.0, 555.6, 611.1, 666.7, 722.2, 777.8, 833.3, 888.9, 944.4, 1000.0}
dsHCV^{A15}, 65°C, Mg^{2+}, Bruker 600 MHz [(a)]	
A15(C8)	[10] {-1000.0, -933.3, -866.7, -800.0, -733.3, -666.7, -600.0, -533.3, -466.7, -400.0, -400.0, -380.5, -361.1, -341.6, -322.1, -302.6, -283.2, -263.7, -244.2, -224.7, -205.3, -185.8, -166.3, -146.8, -127.4, -107.9, -88.4, -68.9, -49.5, -30.0, 30.0, 44.6, 59.2, 73.8, 88.5, 103.1, 117.7, 132.3, 146.9, 161.5, 176.2, 190.8, 205.4, 220.0, 234.6, 249.2, 263.8, 278.5, 293.1, 307.7, 322.3, 336.9, 351.5, 366.2, 380.8, 395.4, 410.0, 424.6, 439.2, 453.8, 468.5, 483.1, 497.7, 512.3, 526.9, 541.5, 556.2, 570.8, 585.4, 600.0, 600.0, 644.4, 688.9, 733.3, 777.8, 822.2, 866.7, 911.1, 955.6, 1000.0} [20] {-1000.0, -933.3, -866.7, -800.0, -733.3, -666.7, -600.0, -533.3, -466.7, -400.0, -400.0, -380.5, -361.1, -341.6, -322.1, -302.6, -283.2, -263.7, -244.2, -224.7, -205.3, -185.8, -166.3, -146.8, -127.4, -107.9, -88.4, -68.9, -49.5, -30.0, 30.0, 44.6, 59.2, 73.8, 88.5, 103.1, 117.7, 132.3, 146.9, 161.5, 176.2, 190.8, 205.4, 220.0, 234.6, 249.2, 263.8, 278.5, 293.1, 307.7, 322.3, 336.9, 351.5, 366.2, 380.8, 395.4, 410.0, 424.6, 439.2, 453.8, 468.5, 483.1, 497.7, 512.3, 526.9, 541.5, 556.2, 570.8, 585.4, 600.0, 600.0, 644.4, 688.9, 733.3, 777.8, 822.2, 866.7, 911.1, 955.6, 1000.0}
dsHCV^{m6A6,A15}, 65°C, Mg^{2+}, Bruker 600 MHz [(a)]	
A15(C8)	[10] {-1000.0, -914.3, -828.6, -742.9, -657.1, -571.4, -485.7, -400.0, -400.0, -380.5, -361.1, -341.6, -322.1, -302.6, -283.2, -263.7, -244.2, -224.7, -205.3, -185.8, -166.3, -146.8, -127.4, -107.9, -88.4, -68.9, -49.5, -30.0, 30.0, 44.0, 58.0, 72.0, 86.0, 100.0, 100.0, 110.3, 120.5, 130.8, 141.0, 151.3, 161.5, 171.8, 182.1, 192.3, 202.6, 212.8, 223.1, 233.3, 243.6, 253.8, 264.1, 274.4, 284.6, 294.9, 305.1, 315.4, 325.6, 335.9, 346.2, 356.4, 366.7, 376.9, 387.2, 397.4, 407.7, 417.9, 428.2, 438.5, 448.7, 459.0, 469.2, 479.5, 489.7, 500.0, 500.0, 600.0, 700.0, 800.0, 900.0, 1000.0}

	[20] {-1000.0, -914.3, -828.6, -742.9, -657.1, -571.4, -485.7, -400.0, -400.0, -380.5, -361.1, -341.6, -322.1, -302.6, -283.2, -263.7, -244.2, -224.7, -205.3, -185.8, -166.3, -146.8, -127.4, -107.9, -88.4, -68.9, -49.5, -30.0, 30.0, 44.0, 58.0, 72.0, 86.0, 100.0, 100.0, 110.3, 120.5, 130.8, 141.0, 151.3, 161.5, 171.8, 182.1, 192.3, 202.6, 212.8, 223.1, 233.3, 243.6, 253.8, 264.1, 274.4, 284.6, 294.9, 305.1, 315.4, 325.6, 335.9, 346.2, 356.4, 366.7, 376.9, 387.2, 397.4, 407.7, 417.9, 428.2, 438.5, 448.7, 459.0, 469.2, 479.5, 489.7, 500.0, 500.0, 600.0, 700.0, 800.0, 900.0, 1000.0}

(a) [NaCl] = 100 mM

Supplementary Table 7. Hybridization $\Delta G^{\ominus}$ from UV melting and NMR CEST

	$\Delta G^{\ominus}$ from UV melting	$\Delta G^{\ominus}$ from NMR CEST
A_6-DNA 45°C	-6.6±0.1	-7.8±0.1
A_6-DNA 50°C	-5.2±0.2	-6.4±0.1
A_2-DNA 50°C	-7.8±0.1	-8.3±0.1
dsGGACU 65°C no Mg^{2+}	-6.3±0.1	-7.7±0.1
$dsGGACU^{m6A}$ 65°C no Mg^{2+}	-5.3±0.1	-6.4±0.1
dsGGACU 65°C Mg^{2+}	-9.3±0.2	-10.1±0.1
$dsGGACU^{m6A}$ 65°C Mg^{2+}	-8.6±0.1	-8.6±0.1
dsHCV 60°C Mg^{2+}	-7.0±0.1	-8.2±0.1
$dsHCV^{m6A}$ 60°C Mg^{2+}	-6.4±0.2	-6.9±0.1

Reference

1. Longhini, A. P.; LeBlanc, R. M.; Becette, O.; Salguero, C.; Wunderlich, C. H.; Johnson, B. A.; D'Souza, V. M.; Kreutz, C.; Dayie, T. K., Chemo-enzymatic synthesis of site-specific isotopically labeled nucleotides for use in NMR resonance assignment, dynamics and structural characterizations. *Nucleic Acids Res.* **2016,** *44* (6).
2. Zimmer, D. P.; Crothers, D. M., NMR of enzymatically synthesized uniformly 13C15N-labeled DNA oligonucleotides. *P Natl Acad Sci USA* **1995,** *92* (8), 3091-3095.
3. Nikolova, E. N.; Kim, E.; Wise, A. A.; O'Brien, P. J.; Andricioaei, I.; Al-Hashimi, H. M., Transient Hoogsteen base pairs in canonical duplex DNA. *Nature* **2011,** *470* (7335), 498-502.
4. Zhou, H.; Kimsey, I. J.; Nikolova, E. N.; Sathyamoorthy, B.; Grazioli, G.; McSally, J.; Bai, T.; Wunderlich, C. H.; Kreutz, C.; Andricioaei, I.; Al-Hashimi, H. M., m1A and m1G disrupt A-RNA structure through the intrinsic instability of Hoogsteen base pairs. *Nat. Struct. Mol. Biol.* **2016,** *23* (9), 803-810.
5. Kimsey, I. J.; Petzold, K.; Sathyamoorthy, B.; Stein, Z. W.; Al-Hashimi, H. M., Visualizing transient Watson-Crick-like mispairs in DNA and RNA duplexes. *Nature* **2015,** *519* (7543), 315-20.
6. Delaglio, F.; Grzesiek, S.; Vuister, G. W.; Zhu, G.; Pfeifer, J.; Bax, A., Nmrpipe - a Multidimensional Spectral Processing System Based on Unix Pipes. *J. Biomol. NMR* **1995,** *6* (3), 277-293.
7. Kimsey, I. J.; Szymanski, E. S.; Zahurancik, W. J.; Shakya, A.; Xue, Y.; Chu, C. C.; Sathyamoorthy, B.; Suo, Z. C.; Al-Hashimi, H. M., Dynamic basis for dG.dT misincorporation via tautomerization and ionization. *Nature* **2018,** *554* (7691), 195-+.
8. Hansen, A. L.; Nikolova, E. N.; Casiano-Negroni, A.; Al-Hashimi, H. M., Extending the range of microsecond-to-millisecond chemical exchange detected in labeled and unlabeled nucleic acids by selective carbon R(1rho) NMR spectroscopy. *J. Am. Chem. Soc.* **2009,** *131* (11), 3818-9.
9. Zhao, B.; Hansen, A. L.; Zhang, Q., Characterizing slow chemical exchange in nucleic acids by carbon CEST and low spin-lock field R(1rho) NMR spectroscopy. *J. Am. Chem. Soc.* **2014,** *136* (1), 20-3.
10. Vallurupalli, P.; Bouvignies, G.; Kay, L. E., Studying "invisible" excited protein states in slow exchange with a major state conformation. *J. Am. Chem. Soc.* **2012,** *134* (19), 8148-61.
11. Rangadurai, A.; Szymaski, E. S.; Kimsey, I. J.; Shi, H.; Al-Hashimi, H. M., Characterizing micro-to-millisecond chemical exchange in nucleic acids using off-resonance R1ρ relaxation dispersion. *Prog. Nucl. Magn. Reson. Spectrosc.* **2019,** *112-113*, 55-102.
12. Bothe, J. R.; Stein, Z. W.; Al-Hashimi, H. M., Evaluating the uncertainty in exchange parameters determined from off-resonance R-1 rho relaxation dispersion for systems in fast exchange. *J. Magn. Reson.* **2014,** *244*, 18-29.
13. Vallurupalli, P.; Sekhar, A.; Yuwen, T. R.; Kay, L. E., Probing conformational dynamics in biomolecules via chemical exchange saturation transfer: a primer. *J. Biomol. NMR* **2017,** *67* (4), 243-271.
14. Hansen, A. L.; Bouvignies, G.; Kay, L. E., Probing slowly exchanging protein systems via

C-13(alpha)-CEST: monitoring folding of the Im7 protein. *J. Biomol. NMR* **2013,** *55* (3), 279-289.
15. Pörschke, D.; Eigen, M., Co-operative non-enzymatic base recognition III. Kinetics of the helix—coil transition of the oligoribouridylic · oligoriboadenylic acid system and of oligoriboadenylic acid alone at acidic pH. *J. Mol. Biol.* **1971,** *62* (2), 361-381.
16. Craig, M. E.; Crothers, D. M.; Doty, P., Relaxation Kinetics of Dimer Formation by Self Complementary Oligonucleotides. *J. Mol. Biol.* **1971,** *62* (2), 383-&.
17. Bloomfield, V. A.; Killman, P. A.; Crothers, D. M.; Tinoco, I.; Hearst, J. E.; Wemmer, D. E.; Turner, D. H., *Nucleic Acids: Structure, Properties, and Functions*. University Science Books: 2000.
18. Rai, R. K.; Tripathi, P.; Sinha, N., Quantification of Metabolites from Two-Dimensional Nuclear Magnetic Resonance Spectroscopy: Application to Human Urine Samples. *Anal. Chem.* **2009,** *81* (24), 10232-10238.
19. Wyer, J. A.; Kristensen, M. B.; Jones, N. C.; Hoffmann, S. V.; Nielsen, S. B., Kinetics of DNA duplex formation: A-tracts versus AT-tracts. *Phys. Chem. Chem. Phys.* **2014,** *16* (35), 18827-39.
20. Siegfried, N. A.; Metzger, S. L.; Bevilacqua, P. C., Folding cooperativity in RNA and DNA is dependent on position in the helix. *Biochemistry* **2007,** *46* (1), 172-181.
21. Liu, B.; Merriman, D. K.; Choi, S. H.; Schumacher, M. A.; Plangger, R.; Kreutz, C.; Horner, S. M.; Meyer, K. D.; Al-Hashimi, H. M., A potentially abundant junctional RNA motif stabilized by m(6)A and Mg(2). *Nat. Commun.* **2018,** *9* (1), 2761.